Neuron
Article

A Glial Signal Consisting of Gliomedin and NrCAM Clusters Axonal Na^+ Channels during the Formation of Nodes of Ranvier

Konstantin Feinberg,[1] Yael Eshed-Eisenbach,[1] Shahar Frechter,[1] Veronique Amor,[1] Daniela Salomon,[1] Helena Sabanay,[1] Jeffrey L. Dupree,[2] Martin Grumet,[3] Peter J. Brophy,[4] Peter Shrager,[5] and Elior Peles[1,*]
[1]Department of Molecular Cell Biology, The Weizmann Institute of Science, Rehovot 76100, Israel
[2]Department of Anatomy and Neurobiology, Virginia Commonwealth University, Richmond, VA 23298, USA
[3]W.M. Keck Center for Collaborative Neuroscience, Rutgers University, Piscataway, NJ 08854, USA
[4]Centre for Neuroscience Research, University of Edinburgh, Edinburgh EH9 1QH, Scotland, UK
[5]Department of Neurobiology and Anatomy, University of Rochester Medical Center, Rochester, NY 14642, USA
*Correspondence: peles@weizmann.ac.il
DOI 10.1016/j.neuron.2010.02.004

SUMMARY

Saltatory conduction requires high-density accumulation of Na^+ channels at the nodes of Ranvier. Nodal Na^+ channel clustering in the peripheral nervous system is regulated by myelinating Schwann cells through unknown mechanisms. During development, Na^+ channels are first clustered at heminodes that border each myelin segment, and later in the mature nodes that are formed by the fusion of two heminodes. Here, we show that initial clustering of Na^+ channels at heminodes requires glial NrCAM and gliomedin, as well as their axonal receptor neurofascin 186 (NF186). We further demonstrate that heminodal clustering coincides with a second, paranodal junction (PNJ)-dependent mechanism that allows Na^+ channels to accumulate at mature nodes by restricting their distribution between two growing myelin internodes. We propose that Schwann cells assemble the nodes of Ranvier by capturing Na^+ channels at heminodes and by constraining their distribution to the nodal gap. Together, these two cooperating mechanisms ensure fast and efficient conduction in myelinated nerves.

INTRODUCTION

Rapid propagation of action potentials along myelinated axons depends on the high-density accumulation of voltage-gated Na^+ channels at regularly spaced interruptions in the myelin known as the nodes of Ranvier (Waxman and Ritchie, 1993). Na^+ channels exist in a complex with the cytoskeletal proteins ankyrin G and βIV spectrin (Berghs et al., 2000), as well as NrCAM and the 186 kDa isoform of neurofascin (NF186), two neural cell adhesion molecules (CAMs) that are enriched at the nodes (Davis et al., 1996; Lambert et al., 1997) and have been implicated in their molecular assembly (Custer et al., 2003; Sherman et al., 2005; Zonta et al., 2008). The nodal complex is formed by multiple molecular interactions between the axonodal CAMs and Na^+ channels (McEwen and Isom, 2004; Ratcliffe et al., 2001) and by the simultaneous binding of these membrane proteins to ankyrin G (Kordeli et al., 1990; Lemaillet et al., 2003; Malhotra et al., 2000).

In the peripheral nervous system (PNS), direct contact between the axon and myelinating Schwann cells is necessary for clustering of the nodal complex (Arroyo et al., 2004; Ching et al., 1999; Dugandzija-Novaković et al., 1995; Saito et al., 2003; Scherer et al., 2001; Tao-Cheng and Rosenbluth, 1983), although the underlying mechanism is not clear (Pedraza et al., 2001; Poliak and Peles, 2003; Salzer et al., 2008; Susuki and Rasband, 2008). During development, Na^+ channel clusters are first detected at heminodes located at the edges of each forming myelin segment (Ching et al., 1999; Schafer et al., 2006; Vabnick et al., 1996). With additional longitudinal growth of the myelin, these heminodal clusters approach each other until two neighboring heminodes fuse, giving rise to a focal node of Ranvier (Dugandzija-Novaković et al., 1995; Vabnick et al., 1996). Throughout this process, myelinating Schwann cells make contact with the axon at two distinct sites: the developing nodes and the adjacent paranodal axoglial junction (PNJ) (Poliak and Peles, 2003; Salzer et al., 2008; Susuki and Rasband, 2008). The PNJs flank the nodes of Ranvier and are formed by an adhesion complex consisting of the glial isoform of neurofascin (NF155) (Tait et al., 2000), and the axonal proteins Caspr (Peles et al., 1997) and contactin (Rios et al., 2000). The PNJ was suggested to function as a barrier to exclude the nodal complex from the internodes (Pedraza et al., 2001; Rosenbluth, 1976). Analysis of mice with disrupted PNJs revealed that while these structures are not essential for the initial clustering of nodal Na^+ channels, they may be important for the long-term maintenance of these channels at the nodal axolemma (Bhat et al., 2001; Boyle et al., 2001; Dupree et al., 1999). In contrast to the PNS, reconstitution of the PNJ in neurofascin null mice by glial expression of NF155 in the CNS is sufficient for clustering Na^+ channels at the nodes of Ranvier (Zonta et al., 2008), further supporting a role for the PNJ in node formation. At the developing, as well as at mature PNS nodes, axoglial contact is formed between Schwann cell microvilli processes and the axolemma (Berthold and Rydmark, 1983; Gatto et al., 2003; Melendez-Vasquez et al., 2001;

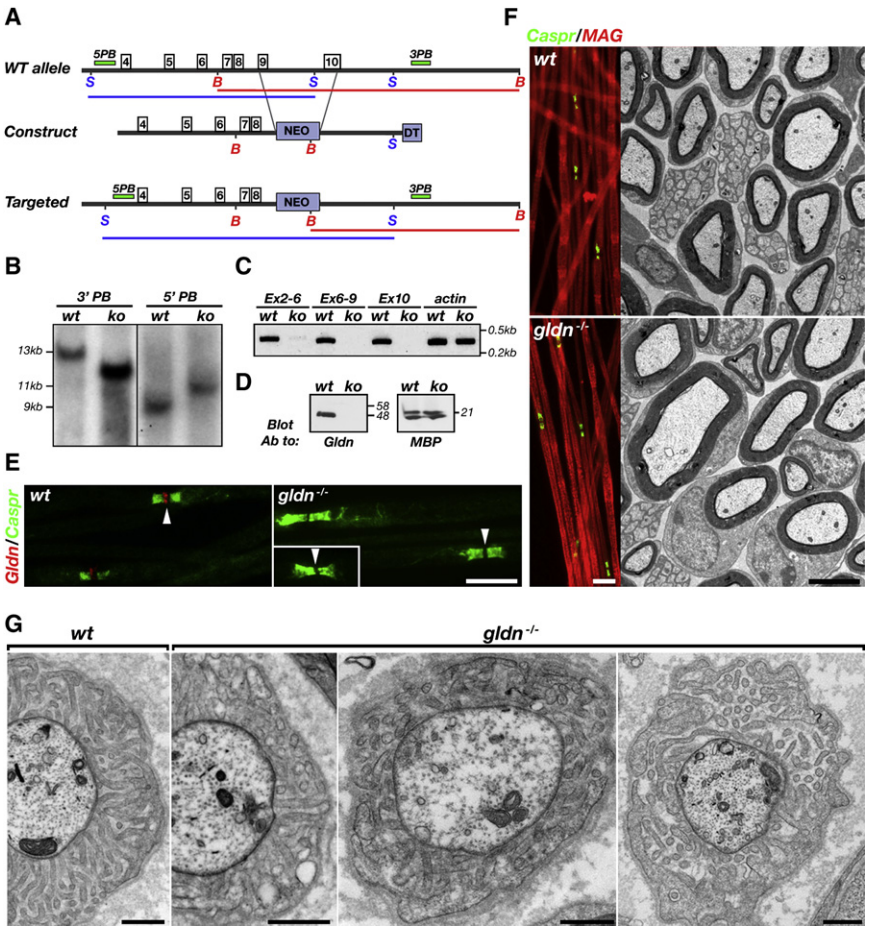

Figure 1. Mice Lacking Gliomedin Exhibit Disorganized Schwann Cell Microvilli

(A) Generation of *gldn*$^{-/-}$ mice. Schematic map of a genomic DNA fragment containing exons 4–10, the targeting construct used and the resulting allele lacking exons 9–10, which encode for the olfactomedin domain of gliomedin. *B*, BglII; *S*, SalI.

(B) Southern blot analysis of genomic DNA of wild-type (wt) or knockout (ko) mice. The location of the probes and the expected fragments are labeled in the first panel.

(C) RT-PCR analysis of DRG mRNA using primer pairs present in exons 2–6 (Ex2–6), 6–9 (Ex6–9), and exon 10 (Ex10) revealed the absence of gliomedin transcript in homozygote mice. Primers for actin were used as controls.

(D) Western blot analysis of sciatic nerve lysates using antibodies to gliomedin (Gldn) or MBP as indicated. The location of molecular mass markers is indicated on the right in kDa.

(E) Gliomedin is absent from nodes in sciatic nerves of *gldn*$^{-/-}$ mice. Teased sciatic nerves of wild-type (wt) and *gldn*$^{-/-}$ mice were labeled using antibodies to gliomedin (Gldn) and Caspr. Inset shows staining of nerves using a different antibody to gliomedin. Arrowheads mark the location of nodes.

(F) Gliomedin null mice exhibit normal PNS myelin. Left panels, immunolabeling of adult sciatic nerves isolated from wt and *gldn*$^{-/-}$ using antibodies to MAG and Caspr. Electron microscopy images of sciatic nerves cross sections are shown on the right panels.

(G) Schwann cell microvilli are disorganized in the absence of gliomedin. Electron microscopy images of sciatic nerves sectioned at nodes of P30 (three left panels) and P12 (right panel) mice. In *gldn*$^{-/-}$ mutant nerves, the microvilli are frequently directed in parallel to the axon and do not contact the axolemma. Scale bars: (E), 10 μm; (F), 10 μm (immunolabeling) and 0.25 μm (EM); (G), 0.5 μm.

Tao-Cheng and Rosenbluth, 1983). This contact is likely mediated by the binding of the multimeric matrix protein gliomedin to both NrCAM and NF186 (Eshed et al., 2007; Eshed et al., 2005). Gliomedin is expressed by myelinating Schwann cells and is concentrated at the edges of the myelin unit with the initial clustering of NF186 and Na^+ channels at heminodes (Eshed et al., 2007; Eshed et al., 2005). Furthermore, in vitro studies indicate that binding of gliomedin may cluster the axonodal CAMs into higher-ordered oligomers, thereby facilitating the recruitment of ankyrin G and Na^+ channels (Dzhashiashvili et al., 2007; Eshed et al., 2007).

To elucidate how Schwann cells control the clustering of Na^+ channels along myelinated axons, we genetically eliminated the expression of gliomedin alone or in combination with other nodal and paranodal adhesion components. We show that gliomedin and NrCAM are glial components of PNS nodes and that together they mediate axon-glia interaction and clustering of Na^+ channels at heminodes by interacting with axonal NF186. Moreover, we show that heminodal clustering of Na^+ channels coincides with a second PNJ-dependent mechanism that constrains their distribution between two myelin segments. Thus, we propose that Schwann cells govern the assembly of PNS nodes by two independent, yet overlapping, adhesion systems to ensure fast conduction in myelinated nerves.

RESULTS

Heminodal Clustering of Na^+ Channels Requires Gliomedin

To examine the role of gliomedin in the assembly of the nodes of Ranvier, we generated gliomedin null mice (Figure 1). Homozygous *gldn*$^{-/-}$ mice display no overt neurological abnormalities and exhibit normal nerve conduction (see Table S1 available online). These mutant mice formed compact PNS myelin that was indistinguishable from their wild-type littermates, but displayed disorganization and impaired attachment of Schwann cell microvilli to the nodal axolemma (Figure 1). As Schwann cell microvilli were implicated in node formation (Gatto et al., 2003; Melendez-Vasquez et al., 2001; Occhi et al., 2005; Saito et al., 2003; Scherer et al., 2001), we examined the distribution of Na^+

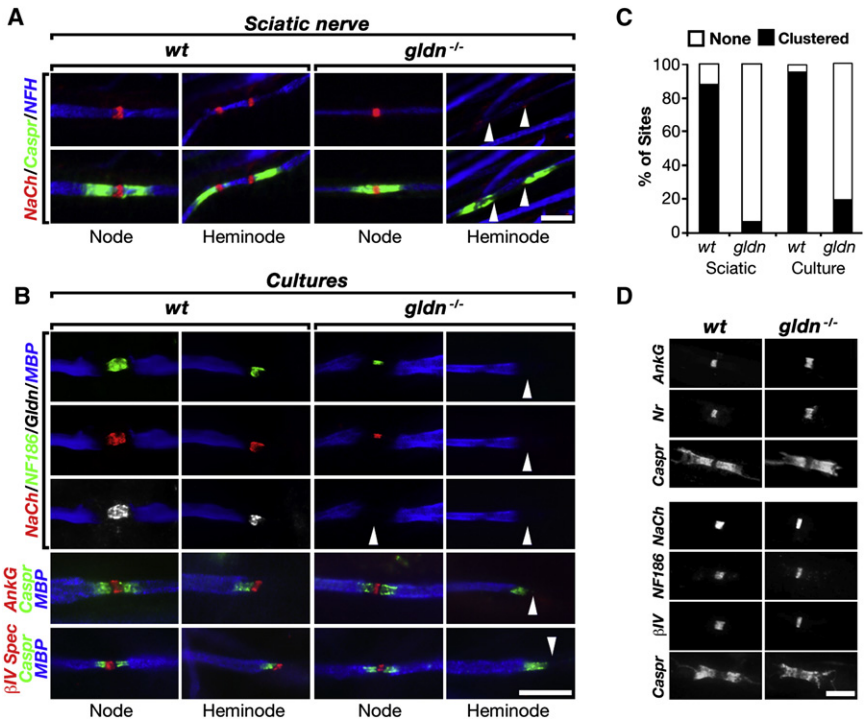

Figure 2. Gliomedin Clusters Na^+ Channels at Heminodes

(A) Na^+ channels are not clustered at heminodes but are present at nodes in *gldn*$^{-/-}$ mice. Sciatic nerve fibers of P6 wild-type (wt) and gliomedin-deficient (*gldn*$^{-/-}$) mice labeled using antibodies to Na^+ channels (NaCh), neurofilament (NFH), and Caspr. For each genotype nodes and heminodes are shown. Arrowheads mark the location of heminodes lacking Na^+ channels.

(B) Myelinated Schwann/DRG neurons cultures isolated from wt and *gldn*$^{-/-}$ mice were labeled with the indicated antibodies. Na^+ channels, NF186, ankyrin G (AnkG), and βIV-spectrin (βIV) are all absent from heminodes in cultures lacking gliomedin (arrowheads). An antibody to MBP was used to label myelin internodes.

(C) Quantification of the appearance of heminodal Na^+ channels in sciatic nerve fibers (Sciatic) or myelinated cultures (SC/DRG) isolated from wt and *gldn*$^{-/-}$ mice; n = 150 sites for sciatic nerves, n = 300 for myelinating cultures ($p < 0.001$).

(D) Nodes of adult *gldn*$^{-/-}$ mice contain all components of the nodal complex. Teased sciatic nerves were labeled with antibodies to Na^+ channels (NaCh), the axonodal CAMs (NrCAM and NF186), and to the nodal cytoskeletal proteins (βIV Spectrin and ankyrin G). An antibody to Caspr was used to mark the paranodal junctions bordering the nodes. Scale bars: (A), 5 μm; (B), 10 μm; (D), 5 μm. See also Figure S1.

channels in the developing sciatic nerves of wild-type and *gldn*$^{-/-}$ at P6, at a time when both nodes and heminodes can be detected (Schafer et al., 2006). We found that in wild-type nerves Na^+ channels were clustered in both mature nodes (i.e., nodes that are flanked by two adjacent Caspr-labeled PNJs) and heminodes, while in *gldn*$^{-/-}$ nerves these channels were absent from heminodes and were only detected in mature nodes (Figure 2A). In adult sciatic nerves of *gldn*$^{-/-}$ mice, Na^+ channels were colocalized at the nodes of Ranvier with NF186, NrCAM, ankyrin G, and βIV spectrin (Figure 2D), Caspr was present at the PNJ and Kv1 channels were localized at the juxtaparanodal region similar to wild-type nerves (Figure S1). As an additional experimental approach, we used myelinating Schwann-dorsal root ganglion (DRG) neurons cultures, which enable the monitoring of the detailed molecular assembly of the nodes in PNS axons (Eshed et al., 2005; Lustig et al., 2001; Melendez-Vasquez et al., 2001; Pedraza et al., 2001). In contrast to wild-type cultures, Na^+ channels, NF186, as well as ankyrin G and βIV spectrin were not clustered at heminodes in *gldn*$^{-/-}$ myelinating cultures (Figure 2B). Notably, while both in vivo (Figure 2A) and in myelinating cultures of wild-type nerves (Figure 2B) heminodes appeared adjacent to Caspr-labeled PNJs, in *gldn*$^{-/-}$ nerves heminodes were absent near Caspr-positive sites, indicating that heminodal clustering is not the result of PNJ formation. We then counted the number of sites in which Na^+ channels were clustered near the edge of a myelin segment (Figure 2C). In *gldn*$^{-/-}$ the majority of Na^+ channels were either absent or diffused (*gldn*$^{-/-}$ culture 92%, nerve 81%) in comparison to wild-type nerves where they were clustered in more than 90% of the sites. These results demonstrate that gliomedin is required for clustering the nodal complex at heminodes during myelination.

NF186 and NrCAM Are Required for Clustering of Na^+ Channels at Heminodes but Not for Their Accumulation in Mature Nodes

The observation that clustering of the nodal complex requires gliomedin prompted us to examine whether this activity is mediated by its two axonodal receptors, NrCAM and NF186 (Eshed et al., 2005). We first examined sciatic nerves of *nrcam*$^{-/-}$ mice, in which Na^+ channel clustering in PNS nodes is delayed (Custer et al., 2003). Immunolabeling of teased sciatic nerves isolated from 6-day-old (P6) mice using antibodies to Na^+ channels and Caspr (to label the PNJs) showed that Na^+ channels were not clustered at heminodes that were already bordered by Caspr-labeled PNJs (Figures 3A and 3D). In addition, Na^+ channels, NF186 and gliomedin were all detected at heminodes in myelinating DRG cultures derived from wild-type, but not from *nrcam*$^{-/-}$ mice (Figures 3B and 3D). In both sciatic nerves and myelinated cultures, Na^+ channels, NF186, gliomedin, ankyrin G, and βIV spectrin were accumulated at mature nodes (Figures 3A and 3B and Table S2). Thus, similar to gliomedin, NrCAM is required for heminodal clustering but not for the accumulation of Na^+ channels at mature nodes of Ranvier.

Genetic ablation of the neuronal (NF186) and glial (NF155) isoforms of neurofascin leads to the disruption of both PNJs and nodes (Sherman et al., 2005). In line with these findings, nodes fail to form in myelinating cocultures of DRG neurons and Schwann cells isolated from *nfasc*$^{-/-}$ mice (Figure S2A). To examine

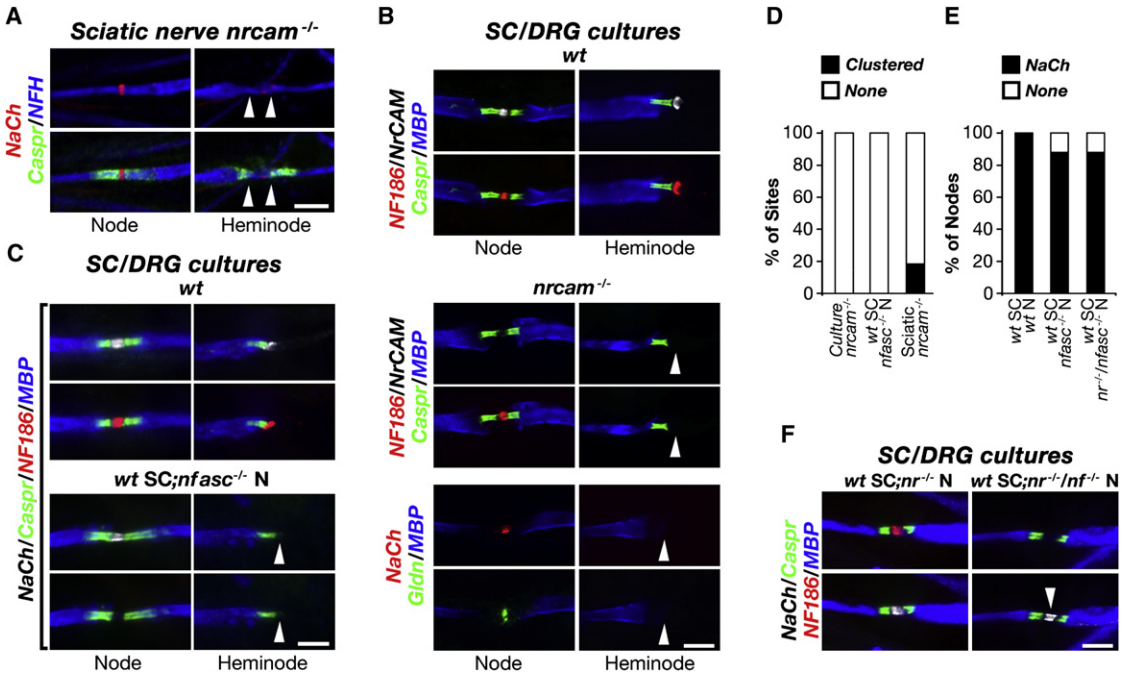

Figure 3. Na^+ Channel Clustering at Heminodes Requires Both NrCAM and NF186

(A) P6 sciatic nerve fibers of *nrcam* null mice ($nrcam^{-/-}$) were labeled using antibodies to Na^+ channels (NaCh), neurofilament (NFH), and Caspr. Arrowheads indicate the absence of Na^+ channel clustering at heminodes.

(B) Myelinated Schwann/DRG neurons cultures isolated from *wt* and $nrcam^{-/-}$ mice were labeled with the indicated antibodies. Na^+ channels, NF186 and gliomedin are absent from heminodes (arrowheads), but are present at mature nodes in $nrcam^{-/-}$ cultures. An antibody to MBP was used to label myelin internodes.

(C) Na^+ channels are not clustered at heminodes in myelinated axons lacking NF186. Wild-type Schwann cells were allowed to myelinate wild-type (wt), or neurofascin null DRG neurons (*wtSC;nfasc*$^{-/-}$*N*). Cultures were immunolabeled using antibodies to MBP, Caspr, Na^+ channels (NaCh), and NF186. In *wtSC;nfasc*$^{-/-}$*N* cultures (which lacks NF186), Caspr is present at the paranodal junction and Na^+ channels accumulate at nodes, but not in heminodes.

(D) Appearance of heminodal Na^+ channel clusters in $nrcam^{-/-}$ sciatic nerve, $nrcam^{-/-}$ myelinated cultures, or cultures containing wt Schwann cells and $nfasc^{-/-}$ neurons (*wtSC;nfasc*$^{-/-}$*N*, i.e., *nf186*$^{-/-}$); n = 150 sites for sciatic nerves, n = 300 for myelinating cultures ($p < 0.001$).

(E) Percentage of mature nodes containing (NaCh), or lacking (none), Na^+ channels in wild-type (wt) myelinated cultures, cultures of wild-type Schwann cells and neurofascin null neurons (*wtSC;nfasc*$^{-/-}$*N*, i.e., *nf186*$^{-/-}$), or cultures of wild-type Schwann cells and neurons isolated from double null mice lacking both NrCAM and neurofascin (*wtSC;nrcam*$^{-/-}$/*nfasc*$^{-/-}$*N*); n = 200 ($p < 0.001$).

(F) Na^+ channels accumulate in mature nodes in the absence of the axonodal CAMs. Myelinating cocultures containing wild-type Schwann cells and DRG neurons isolated from mice lacking NrCAM (*wt*SC;*nr*$^{-/-}$) or both NrCAM and NF186 (*wt*SC;*nf*$^{-/-}$/*nr*$^{-/-}$N), were labeled using the indicated antibodies. Arrowhead marks the presence of Na^+ channels at nodes in the absence of axonal NF186 and NrCAM. Scale bars: 5 μm. See also Figure S2.

directly the role of NF186 in the assembly of PNS nodes, we determined whether Na^+ channels accumulate at nodes in the absence of NF186 by coculturing DRG neurons isolated from *nfasc*$^{-/-}$ mice with wild-type Schwann cells. In agreement with a recent report (Zonta et al., 2008), the expression of NF155 in myelinating Schwann cells promoted the full recovery of the PNJs, as demonstrated by immunolabeling for Caspr (Figure 3C). PNJ formation in these axons was accompanied by the accumulation of Na^+ channels at the nodes together with all other components of the nodal complex (i.e., ankyrin G, βIV spectrin, and NrCAM) except NF186 (Figures 3C, 3E, and S2A and Table S2). However, similarly to gliomedin and NrCAM-deficient DRG cultures, in the absence of axonal NF186, Na^+ channels were not clustered at heminodes (Figures 3C and 3D). To further determine the contribution of the axonodal CAMs to the formation of mature nodes, we established myelinating cultures using DRG neurons isolated from double *nrcam*$^{-/-}$/*nfasc*$^{-/-}$ mutant mice and wild-type Schwann cells (to recover the PNJs). Analysis of these cultures showed that Na^+ channels, as well as ankyrin G and βIV spectrin, accumulated at nodes that were flanked by PNJs, but not at heminodes (Figures 3E and 3F and Table S2). Taken together, these results demonstrate that gliomedin, NrCAM and NF186, are all required for developmental clustering of Na^+ channel at heminodes. Furthermore, these results reveal the existence of an additional mechanism that enables the accumulation of Na^+ channels in mature nodes independently of heminodal clustering and the axonodal CAMs.

Cooperation of NrCAM and Gliomedin as a Glial Signal for Heminodal Clustering

The requirement for both NrCAM and NF186 for Na^+ channel clustering at heminodes by gliomedin is unexpected, given that both axonodal CAMs bind gliomedin (Eshed et al., 2005) and could potentially bind ankyrin G through their remarkably similar cytoplasmic domains (Davis and Bennett, 1994). To further evaluate the exact role of each component of the nodal adhesion

complex in heminodal clustering, we first examined whether binding of gliomedin to axons requires both NrCAM and NF186. We found that the soluble extracellular domain of gliomedin (Gldn-Fc) bound to DRG neurons that had been isolated from wild-type, as well as from *nrcam*$^{-/-}$ and *nfasc*$^{-/-}$, but not from *nrcam*$^{-/-}$/*nfasc*$^{-/-}$ double-mutant embryos (Figure 4A). Thus, NrCAM and NF186 are the only axonal receptors for gliomedin, and the presence of only one of these CAMs is sufficient for gliomedin's binding to the axolemma. We next examined whether binding of gliomedin to axons lacking either NrCAM or NF186 could induce Na^+ channel clustering. Gldn-Fc was incubated with DRG neurons isolated from wild-type, *nrcam*$^{-/-}$ or *nfasc*$^{-/-}$ mice for 48 hr and then fixed and immunolabeled using an antibody to Na^+ channels (Figure 4B). Na^+ channel clustering was only detected along axons derived from wild-type and *nrcam*$^{-/-}$, but not those derived from *nfasc*$^{-/-}$ mice. Interestingly, in node-like clusters that formed by gliomedin in wild-type axons, we could not detect NrCAM using an antibody that recognizes its intracellular domain (Figure 4C), suggesting that the axonal form of NrCAM lacks this domain and is therefore unable to recruit ankyrin G and Na^+ channels. Taken together, these results demonstrate that although both NrCAM and NF186 bind to gliomedin, only NF186 is able to recruit Na^+ channels. In line with this observation, we found that Na^+ channels do not cluster at heminodes in the absence of NF186, despite the presence of NrCAM and gliomedin at these sites (Figure S2B).

These results raise the question of what might be the role of NrCAM, which is expressed by a variety of neurons and glial cells (Grumet, 1997; Suter et al., 1995), in heminodal clustering. RT-PCR analysis revealed the presence of an NrCAM transcript in purified rat and mouse Schwann cells, as well as in DRG neurons (Figure 5A). Immunoprecipitation and western blot analysis of cultured Schwann cells using an antibody to the extracellular domain of NrCAM demonstrated that Schwann cells express both transmembrane and secreted forms of NrCAM (Figure 5B). This result is in line with previous observations detecting a cleavage product comprising the entire extracellular domain of NrCAM in the nervous system (Kayyem et al., 1992; Davis et al., 1996). Since both neurons and Schwann cells express NrCAM, we set out to determine the relative contributions of NrCAM expressed by each cell type to Na^+ channels clustering at nodes and heminodes. In contrast to wild-type cultures, in *nrcam*$^{-/-}$ cultures heminodes were not formed (see also Figure 3). Culturing Schwann cells derived from *nrcam*$^{-/-}$ mice with wild-type DRG neurons, resulted in the appearance of normal nodes containing Na^+ channels, NF186 and NrCAM (Figure 5C and Table S2). However, these molecules were not clustered at heminodes that were located along the same myelinated axon, demonstrating that NrCAM of neuronal origin is unable to promote Na^+ channel clustering at heminodes. We next examined whether glial NrCAM is required for heminodal clustering of Na^+ channels by coculturing DRG neurons derived from *nrcam*$^{-/-}$ mice with wild-type Schwann cells. Remarkably, NrCAM, Na^+ channels, NF186 and gliomedin were all present at heminodes (90% of sites, n = 160) in these cultures (Figure 5D). Immunolabeling of similar cultures with antibodies to the cytoplasmic and extracellular domains of NrCAM, revealed the presence of the transmembrane form of glial NrCAM at heminodes and mature nodes (Figure S3A). Finally, to determine whether NrCAM also affects the interaction of gliomedin with axons, we examined the binding of gliomedin to DRG neurons in the

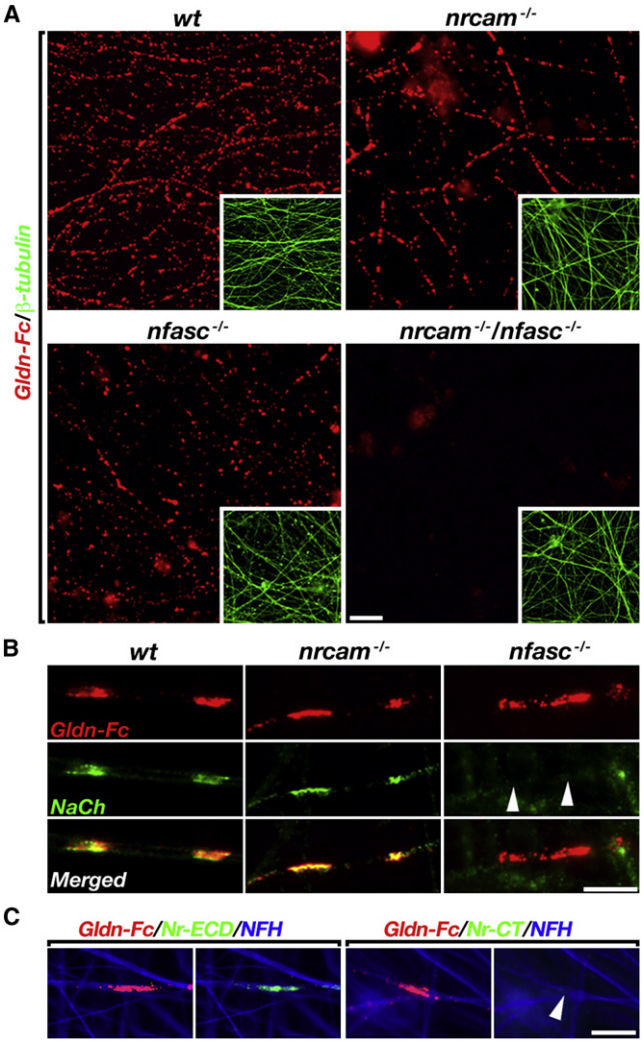

Figure 4. Gliomedin-Dependent Na^+ Channel Clustering Is Mediated by NF186

(A) Gliomedin binds to both NF186 and NrCAM. Binding of soluble Fc-fusion protein containing the extracellular domain of gliomedin (Gldn-Fc) to DRG neurons isolated from wild-type (wt), *nrcam*$^{-/-}$, *nfasc*$^{-/-}$ or double *nrcam*$^{-/-}$/*nfasc*$^{-/-}$ mutant mice. The presence of neurons was monitored by immunolabeling for βIII-tubulin (shown at lower magnification in insets). Note the absence of Gldn-Fc binding to DRG neurons lacking both NF186 and NrCAM.

(B) Na^+ channel clustering requires NF186 but not NrCAM. Gldn-Fc was mixed with Cy3-conjugated secondary antibody to human Fc, and incubated with DRG neurons for 48 hr before fixing. Binding of Gldn-Fc is shown in the upper panels, along with immunofluorescence labeling for Na^+ channels (NaCh) and the merged images. Arrowheads indicate the absence of Na^+ channel clusters in *nfasc*$^{-/-}$ neurons.

(C) NrCAM clustered by gliomedin lacks its intracellular domain. DRG neurons were incubated with Gldn-Fc as described above and then fixed and immunolabeled using an antibody to neurofilament (NFH) together with antibodies that recognize the extracellular (NrCAM-ECD), or intracellular (NrCAM-Cyto) domain of NrCAM. Arrowhead depicts the absence of the intracellular domain of NrCAM in the cluster. Scale bars, 10 μm.

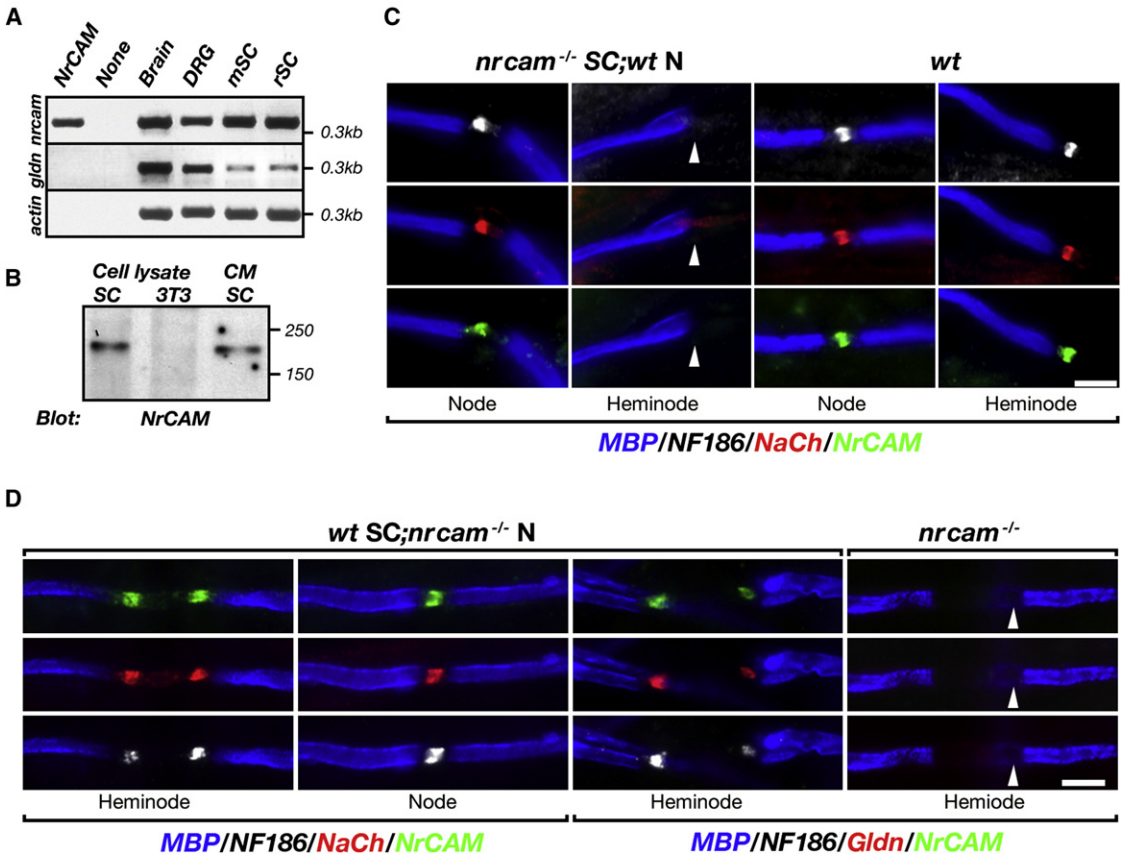

Figure 5. NrCAM and Gliomedin Provide a Glial Signal for Na^+ Channel Clustering

(A) NrCAM is expressed by Schwann cells. RT-PCR analysis using primers for *nrcam*, *gldn*, or *actin* on mRNA isolated from brain, mixed DRG/SC culture (DRG), and isolated mouse (mSC) or rat (rSC) Schwann cells. NrCAM cDNA (NrCAM) and reaction mix without template (none) were used as positive and negative controls, respectively.

(B) Schwann cells express a transmembrane and a secreted form of NrCAM. Cell lysates of Schwann cells and control 3T3 fibroblasts or the growth medium of cultured Schwann cells were subjected to immunoprecipitation and western blot analysis using an antibody to the extracellular domain of NrCAM. The location of molecular mass markers is indicated on the right in kDa.

(C) Neuronal expression of NrCAM is not sufficient for heminodal Na^+ channel clustering. Myelinating cultures were prepared using wild-type Schwann cells and DRG neurons (wt), or $nrcam^{-/-}$ Schwann cells and wild-type neurons ($nrcam^{-/-}$ SC; wt N). In the absence of glial NrCAM (i.e., in $nrcam^{-/-}$ SC; wt N cultures), NF186, Na^+ channels (NaCh) and axonal NrCAM accumulated in mature nodes, but did not clustered in heminodes (arrowheads).

(D) Glial NrCAM induces heminodal clustering of Na^+ channels. Myelinating $nrcam^{-/-}$ cultures, or cultures prepared using $nrcam^{-/-}$ neurons and wild-type Schwann cells (wt SC; $nrcam^{-/-}$ N) were immunolabeled using the indicated antibodies. In contrast to $nrcam^{-/-}$ cultures (arrowheads), in wt SC; $nrcam^{-/-}$ N cultures, glial NrCAM clustered at heminodes together with NF186, Na^+ channels (NaCh) and gliomedin (Gldn). Scale bars, 5 μm. See also Figure S3.

presence or absence of the extracellular domain of NrCAM. While soluble NrCAM alone did not bind neurons, its presence enhanced the binding of gliomedin to these cells (Figure S3B). This effect was specific to NrCAM and was not observed using the extracellular domain of NF186. Taken together, these results demonstrate that NrCAM expressed by Schwann cells, rather than neurons, is required for Na^+ channels clustering at heminodes. They further suggest that glial NrCAM plays a dual role in heminodal clustering by trapping gliomedin on the Schwann cell microvilli, and by enhancing its binding to NF186.

Involvement of the PNJ in Node Formation

Our results demonstrate that even in the absence of gliomedin (Figure 2), NrCAM (Figure 3B), or NF186 (Figure 3C), Na^+ channels were eventually accumulated at mature nodes. One possible mechanism that could operate in the absence of heminodal clustering might be provided by the PNJ (Rosenbluth, 2009). This specialized axon-glial contact serves as a membrane barrier separating juxtaparanodal K^+ channels from Na^+ channels at the nodes but its role in the assembly of the nodes of Ranvier remains unclear. Myelinating DRG cultures lacking gliomedin, NrCAM or NF186, in which heminodes fail to form, allowed us to directly examine the role of the PNJ in the assembly of PNS nodes. As demonstrated in Figure 6A, in wild-type cultures Na^+ channels were clustered at heminodes, which eventually merged, forming a mature focal node of Ranvier. In contrast, in $gldn^{-/-}$ and $nrcam^{-/-}$ cultures, as well as in cultures containing $nfasc^{-/-}$ neurons and wild-type Schwann cells (i.e., thus considered as $nf186^{-/-}$), Na^+ channels were accumulated between the two approaching myelin segments. This Na^+

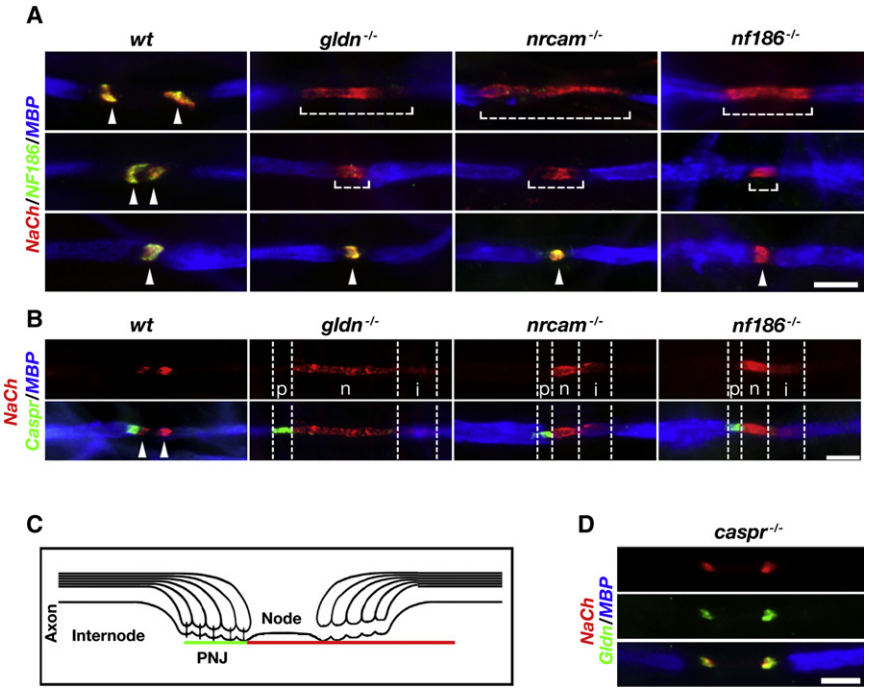

Figure 6. The PNJ Restrict the Area Occupied by Na^+ Channels between Two Myelin Segments

(A) Developmental stages of node formation. Myelinated Schwann cell/DRG neurons cultures obtained from wild-type (wt), *gldn*$^{-/-}$ and *nrcam*$^{-/-}$ mice, or myelinating cocultures consisting of wild-type Schwann cells and DRG neurons isolated from *nfasc*$^{-/-}$ mice (*nf186*$^{-/-}$) were labeled using antibodies to Na^+ channels (NaCh), NF186, and MBP. Merged images of three different stages of the developing nodal gaps found in the same culture. Arrowheads indicate both heminodes and nodes. In the absence of either gliomedin, NrCAM, or NF186, Na^+ channels are initially scattered between two distant myelin segments and then accumulate at mature nodes. Note that in *gldn*$^{-/-}$ and *nrcam*$^{-/-}$ cultures, NF186 is missing from the area occupied by scattered Na^+ channels, but emerges later in mature nodes.

(B) Na^+ channels invade the internodal region below the compact myelin in the absence of PNJ. Myelinated cultures of the indicated genotypes were immunolabeled using antibodies to Na^+ channels (NaCh), Caspr (to mark the PNJ), and MBP (to label compact myelin). Images show examples of nodal gaps that are bordered by the PNJ only on one side. The location of the paranodes (p), nodes (n), and internodes (i) is marked by vertical dashed lines. Arrowheads marks heminodal clustering of Na^+ channels in wild-type cultures.

(C) Scheme illustrating the distribution of Na^+ channels (red) and Caspr (green) detected in (B).

(D) Heminodes are formed in the absence of PNJ. Na^+ channels cocluster with gliomedin at heminodes in myelinated cultures of Schwann cell/DRG neurons isolated from *caspr*$^{-/-}$ mice. Scale bars: (A–D), 5 μm. See also Figure S4.

channel immunoreactivity was more pronounced as the nodal gap narrowed down until it formed a mature node. Notably, while in isolated heminodes in *gldn*$^{-/-}$ and *nrcam*$^{-/-}$ cultures (Figures 2B and 3B) diffuse Na^+ channels immunoreactivity was only detected in ~30% of the sites, these channels were always detected at the nodal gap as two myelin segments approached each other (Figure 6A). A similar distribution of Na^+ channels was detected in developing sciatic nerves of *gldn*$^{-/-}$ and *nrcam*$^{-/-}$ nerves (Figure S4). Interestingly, although Na^+ channels coclustered with NF186 during all developmental stages in wild-type cultures, NF186 was not detected in *gldn*$^{-/-}$ and *nrcam*$^{-/-}$ cultures until these channels were already accumulated at focal nodes (Figure 6A), providing an additional indication that the accumulation of Na^+ channels in mature nodes could occur independently of the axonodal CAMs. To further examine the role of the PNJ in node formation, we searched for sites in which the PNJ (identified by Caspr immunoreactivity) was formed at only one side of the nodal gap (i.e., PNJ was formed by one myelin segment but not the other). Analysis of these sites allowed us to examine the distribution of Na^+ channels along the same myelinated axon in the presence or absence of the PNJ. Immunolabeling of *gldn*$^{-/-}$, *nrcam*$^{-/-}$, and *nf186*$^{-/-}$ cultures using antibodies to Caspr, Na^+ channels, and MBP, showed that Na^+ channels were eliminated from the area occupied by the PNJ, but invaded the axolemma underneath the myelin sheath in its absence (Figures 6B and 6C). These observations suggest that in addition to being actively clustered at heminodes, Na^+ channels are constrained between two neighboring myelin segments by the PNJ. Furthermore, in the absence of the PNJ, as found in mice lacking Caspr for example, the presence of gliomedin and the axonodal CAMs enable the clustering of Na^+ channels at heminodes and consequently in mature nodes (Figure 6D).

Heminodal Clustering and the PNJ Provide Reciprocal Backup Systems for Node Formation

To test whether axoglial contact at both heminode and the PNJ contribute to the formation of the nodes of Ranvier, we generated *gldn*$^{-/-}$/*caspr*$^{-/-}$ and *nrcam*$^{-/-}$/*caspr*$^{-/-}$ mice. In agreement with previous reports (Bhat et al., 2001; Gollan et al., 2003), *caspr* null mice exhibit progressive neurological defects that were already apparent at P11, but nevertheless have a normal life span. Both homozygous *gldn*$^{-/-}$/*caspr*$^{-/-}$ and *nrcam*$^{-/-}$/*caspr*$^{-/-}$ mice exhibit dramatic proprioceptive and motor deficits that appear earlier (*gldn*$^{-/-}$/*caspr*$^{-/-}$ at P5-6, and *nrcam*$^{-/-}$/*caspr*$^{-/-}$ at P3–4) and are more severe than in the single *caspr*$^{-/-}$ mutant mice (Bhat et al., 2001; Gollan et al., 2003; Table S1). Double *nrcam*$^{-/-}$/*caspr*$^{-/-}$ and *gldn*$^{-/-}$/*caspr*$^{-/-}$ mice died at P8 and P14, respectively. Sciatic nerves isolated from *gldn*$^{-/-}$/*caspr*$^{-/-}$ and *nrcam*$^{-/-}$/*caspr*$^{-/-}$ pups had myelin that was indistinguishable from their single mutant littermates or wild-type control animals (Figure S5A). However, in both homozygous mutants, Schwann cell microvilli were disorganized, did not attach the nodal axolemma and often penetrated the space between the paranodal loops and the axolemma (Figure S5A). Immunofluorescence analysis of P6 sciatic

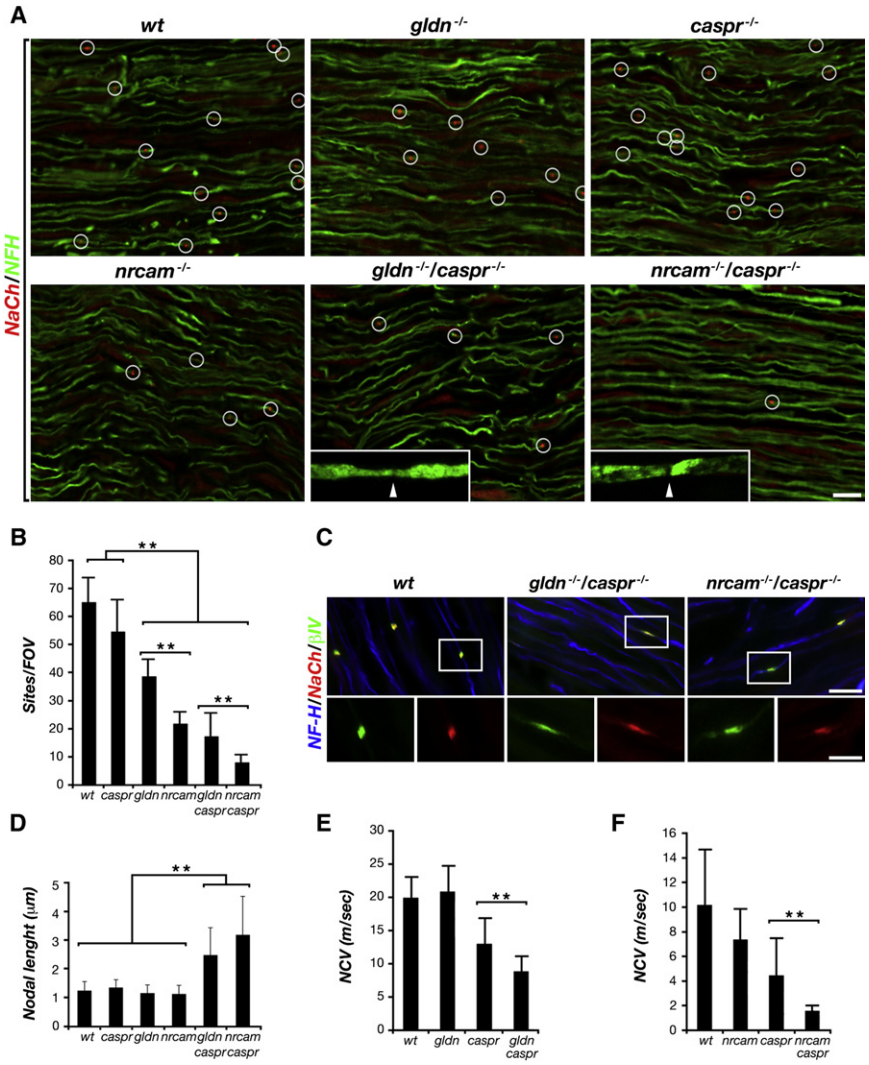

Figure 7. Assembly of the Nodes of Ranvier Requires Axoglial Contacts at Nodes and Paranodes

(A) A reduction in Na^+ channel clustering in *gldn*$^{-/-}$/*caspr*$^{-/-}$ and *nrcam*$^{-/-}$/*caspr*$^{-/-}$ mice. Longitudinal sections of P6 sciatic nerves isolated from the indicated genotypes, immunolabeled with antibodies to neurofilament (*NFH*) and Na^+ channels (*NaCh*). Higher magnification of representative nodal sites lacking Na^+ channels (arrowheads) in sciatic nerves of the double mutants is shown in the lower panels.

(B) Amount of Na^+ channels clusters per field of view (FOV); error bars, SD of n = 15–20 fields for each genotype (**p < 0.001).

(C) Examples of nodal sites that formed in *gldn*$^{-/-}$/*caspr*$^{-/-}$ and *nrcam*$^{-/-}$/*caspr*$^{-/-}$ mice. P6 sciatic nerves isolated from wild-type (wt), *gldn*$^{-/-}$/*caspr*$^{-/-}$, and *nrcam*$^{-/-}$/*caspr*$^{-/-}$ mice were immunolabeled using antibodies to neurofilament (*NFH*), Na^+ channels (*NaCh*), and βIV spectrin (βIV). Higher magnification of the boxed area is shown below each panel.

(D) Quantification of the areas occupied by Na^+ channels colocalized with βIV spectrin in the different genotypes; error bars, SD of n = 100 sites for each genotype (**p < 0.001).

(E and F) Nerve conduction velocity (NCV) is reduced in double mutant mice lacking Caspr and either gliomedin or NrCAM. Compound action potentials were recorded from sciatic nerves of P14 (E) or P7 (F) animals; error bars, SEM of n = 7 mice for each genotype (**p < 0.005). Scale bars: (A), 10 μm; (C), 5 μm. See also Figure S5.

nerves revealed that the total amount of Na^+ channel clusters formed in *gldn*$^{-/-}$/*caspr*$^{-/-}$ and *nrcam*$^{-/-}$/*caspr*$^{-/-}$ nerves was considerably reduced, reaching only 26% and 12%, respectively of their wild-type age-matched littermates (Figures 7A and 7B). Since in both *gldn*$^{-/-}$ and *nrcam*$^{-/-}$ mice heminodes do not form, and given that the formation of mature nodes is delayed in *nrcam*$^{-/-}$ mice (Custer et al., 2003), the number of Na^+ clusters in *gldn*$^{-/-}$ and *nrcam*$^{-/-}$ nerves at this age only reached 59% and 33% of their wild-type controls, respectively. Nevertheless, further genetic ablation of Caspr in both *gldn*$^{-/-}$ and *nrcam*$^{-/-}$ mice resulted in an additional ~40% (45% and 36%, respectively) reduction in the number of Na^+ channels. In both *gldn*$^{-/-}$/*caspr*$^{-/-}$ and *nrcam*$^{-/-}$/*caspr*$^{-/-}$ mutant nerves, the total amount of Na^+ channels had not been changed as determined by western blot analysis (Figure S5B). Furthermore, nodal Na^+ channel that were still detected in *gldn*$^{-/-}$/*caspr*$^{-/-}$ and *nrcam*$^{-/-}$/*caspr*$^{-/-}$ mice were frequently abnormal and wider than those of wild-type or *gldn*$^{-/-}$, *caspr*$^{-/-}$, or *nrcam*$^{-/-}$ single mutant nerves (Figures 7C and 7D). Electrophysiological analysis of sciatic nerves dissected from P14 *gldn*$^{-/-}$/*caspr*$^{-/-}$ and P7 *nrcam*$^{-/-}$/*caspr*$^{-/-}$ animals showed a striking reduction in conduction velocity (Figures 7E and 7F and Table S1). Taken together, these results indicate that node formation in the PNS is achieved by the clustering of Na^+ channels at heminodes as well as by constraining their distribution to the nodal gap by the PNJ.

DISCUSSION

The propagation of action potentials in myelinated axons requires the precise localization of Na^+ channels at the nodes of Ranvier. The accumulation of Na^+ channels at nodes depends on the presence of intact myelinating glial cells, as evidenced by their abnormal distribution and reduced nerve conduction in demyelinating diseases (Coman et al., 2006; Craner et al., 2003; Lonigro and Devaux, 2009). Here, we provide new insights into the mechanisms that regulate the formation of the nodes of Ranvier in the PNS. We report that myelinating Schwann cells control the molecular assembly of nodes by two distinct mechanisms: (1) clustering Na^+ channels at heminodes and (2) restricting their distribution between two myelinating segments. These two mechanisms require different adhesion complexes, each of which mediate distinct axon-glia interactions at the developing nodes and the paranodes (Figure 8).

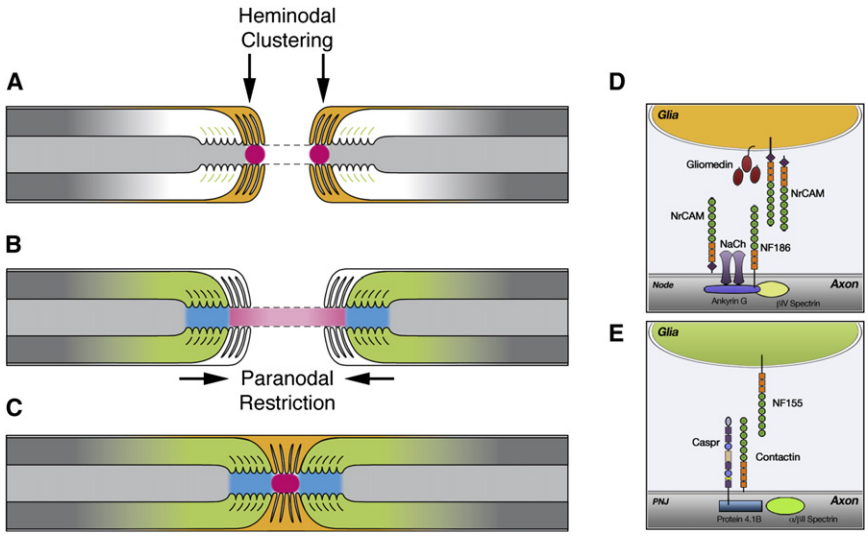

Figure 8. Two Distinct Axoglial Adhesion Systems Assemble PNS Nodes of Ranvier

(A) Na^+ channels (red circle) are trapped at heminodes that are contacted by Schwann cell microvilli (MV; orange). Axon-glia interaction at this site is mediated by binding of gliomedin and glial NrCAM to axonal NF186 (D). A transmembrane and secreted forms of glial NrCAM trap gliomedin on Schwann cell microvilli and enhances its binding to NF186. In the absence of either gliomedin or glial NrCAM, Na^+ channels fail to cluster at heminodes. Binding of gliomedin to axonal NrCAM, which lack its cytoplasmic domain does not result in Na^+ channel clustering.

(B) The distribution of Na^+ channels is restricted between two forming myelin segments by the PNJ (blue). Three CAMs, NF155 present at the paranodal loops (green) and axonal complex of Caspr and contactin mediate axon-glia interaction and the formation of the PNJ (E).

(C) These two cooperating mechanisms provide reciprocal backup systems and ensure that Na^+ channels are found at high density at the nodes.

Role of Gliomedin and NF186 in Heminodal Clustering of Na^+ Channels

An important outcome of this study is the distinction between the underlying molecular mechanisms operating during heminodal clustering and the PNJ-dependent accumulation of Na^+ channels at mature nodes. Surprisingly, we found that although heminodes are regarded as early precursors of nodes, Na^+ channels could eventually accumulate at mature nodes even in the absence of heminodal clustering. We demonstrate that Schwann cell-mediated Na^+ channel clustering at heminodes requires gliomedin, NrCAM and NF186. In the absence of any one of these nodal adhesion components, Na^+ channels, as well as ankyrin G and βIV spectrin, are not clustered at heminodes, but rather are dispersed throughout the forming nodal gap. These results support our previous observations in vitro, demonstrating that gliomedin provides a glial signal for Na^+ channel clustering (Eshed et al., 2005). Previously, we, and others, reported that silencing expression of either gliomedin or NF-186 using RNAi inhibits node formation. However, in those studies nodes and heminodes were routinely counted interchangeably (Eshed et al., 2005; Dzhashiashvili et al., 2007). Thus, the conclusion that gliomedin and NF186 are required for node formation was based on the analysis of heminodes and not mature nodes. In the present study we show that genetic ablation of either gliomedin or NF186 results in the inhibition of the developmental clustering of Na^+ channel at heminodes, but not in the eventual accumulation of these channels at mature nodes. Several lines of evidence indicate that NF186 is the functional axonal receptor for gliomedin. First, binding of gliomedin to axons expressing NF186 but not NrCAM (i.e., *nrcam*$^{-/-}$ axons) induces the formation of node-like clusters. Second, Na^+ channels are clustered (together with NF186) at heminodes in myelinating cultures containing wild-type Schwann cells and *nrcam*$^{-/-}$ neurons. Third, although gliomedin and NrCAM are present at heminodes in the absence of neurofascin, their presence is not sufficient for clustering of Na^+ channels at these sites. In contrast to NF186, the role of axonal NrCAM is less clear. We found that although gliomedin could bind to axonal NrCAM in the absence of NF186 (i.e., *nfasc*$^{-/-}$ axons), it did not induce nodal-like clusters of ankyrin G and Na^+ channels. Furthermore, we show that the NrCAM that was present in these clusters lacked its intracellular domain, which is required for its interaction with ankyrin G. It is currently unknown whether the axonal NrCAM lacking the cytoplasmic domain is produced by alternative splicing or by proteolytic cleavage of the transmembrane protein. Our results indicate that although NrCAM is present in axons together with NF186, it is the latter CAM that serves as the axonal receptor that mediates heminodal clustering of Na^+ channels by gliomedin.

Glial NrCAM Traps Gliomedin on the Schwann Cell Microvilli

How does gliomedin, which is released from Schwann cells by proteolytic cleavage of furin and BMP proteases (Eshed et al., 2007; Maertens et al., 2007), get recruited to Schwann cell processes that contact heminodes? Surprisingly, the localization of gliomedin at heminodes depends on glial NrCAM, which until now was thought to be exclusively an axonodal CAM (Salzer et al., 2008). Using myelinating cultures containing wild-type Schwann cells and *nrcam*$^{-/-}$ neurons, we found that a transmembrane form of NrCAM is present at the Schwann cell microvilli. Furthermore, myelinating cultures prepared using different combinations of DRG neurons and Schwann cells isolated from wild-type and *nrcam*$^{-/-}$ mice, revealed that heminodal clustering of Na^+ channels requires glial and not axonal NrCAM. These results provide an explanation for why heminodal clustering does not occur in *nrcam*$^{-/-}$ nerves, which express gliomedin that could potentially induce Na^+ channel clustering through NF186. In accordance, gliomedin was absent from heminodes in *nrcam*$^{-/-}$ nerves and cultures, and reappeared at these sites when the expression of glial NrCAM was restored in mixed cultures containing wild-type Schwann cells. In addition to the role of glial NrCAM in localizing gliomedin to the edge of the forming myelin segments, we found that NrCAM enhances the binding of gliomedin to NF186. Together, these findings

reveal a previously unrecognized role for NrCAM in node formation as a glial signal with gliomedin. The extracellular region of gliomedin contains olfactomedin and collagen domains, which enable its simultaneous interaction with both NrCAM and NF186, as well as with extracellular matrix proteoglycans (Eshed et al., 2005, 2007). Although the exact mechanism is yet to be determined, glial NrCAM may increase the local concentration of gliomedin multimers, thereby enhancing its binding and clustering of NF186. We propose that during myelination, glial NrCAM tethers gliomedin to Schwann cell microvilli. This NrCAM/gliomedin complex serves as a Schwann cell signal for Na^+ channel clustering at heminodes by binding to axonal NF186. These initial clusters serve as a local nucleating center at the axolemma to which Na^+ channels and ankyrin G are recruited. In agreement, heminodal clustering of Na^+ channels requires that the ankyrin G-binding site be present in the cytoplasmic region of NF186 (Dzhashiashvili et al., 2007).

The Paranodal Axoglial Junctions Constrain Na^+ Channels between Two Myelin Segments

At both CNS and PNS axons, the PNJs form a membrane barrier that separates the juxtaparanodal Kv1 channels from the nodal area (Salzer et al., 2008). In the CNS, PNJs appear prior to nodes (Rasband et al., 1999), are important for their maintenance (Rios et al., 2003), and, as recently demonstrated, are sufficient for their formation (Zonta et al., 2008). However, their role in PNS node formation has remained uncertain given that Na^+ channel clustering was only minimally affected in mice lacking either Caspr, contactin or NF155 (Bhat et al., 2001; Boyle et al., 2001; Pillai et al., 2009). Our data reveal an additional, PNJ-dependent mechanism for node formation. First, in the absence of heminodal clustering in *gldn*$^{-/-}$ and *nrcam*$^{-/-}$ mice, Na^+ channels eventually accumulate at mature nodes. Second, Na^+ channels invade beneath the compact myelin at sites lacking Caspr, indicating that the PNJs restrict the distribution of these channels to the forming nodal gap. Third, recovery of the PNJ in myelinating cultures of wild-type Schwann cells and *nfasc*$^{-/-}$ neurons lead to the accumulation of Na^+ channels, ankyrin G, βIV spectrin, and NrCAM at nodes. Notably, PNS nodes do not form in *nfasc*$^{-/-}$ mice expressing a cytoplasmic-domain-deleted or tagged versions of NF155 in Schwann cells (Sherman et al., 2005; Zonta et al., 2008), suggesting that the restriction of these channels to PNS nodes by the PNJ may depend on well-timed interactions between the paranodal adhesion complex and the specialized cytoskeleton present at this site (Ogawa et al., 2006). Fourth, genetic removal of both nodal and paranodal adhesion complexes resulted in a marked reduction in node formation. We further show that, in contrast to the process of heminodal clustering, the accumulation of these channels at the axolemma by the PNJ does not require NF186 and NrCAM. These results may explain recent findings, showing that in an experimental model of Guillain-Barre syndrome, many nodes lacking gliomedin and NF186 still maintained normal Na^+ channel clusters in early stages of the disease before paranodal demyelination occurred (Coman et al., 2006; Craner et al., 2003; Lonigro and Devaux, 2009). How the PNJ restricts the distribution of Na^+ channels is presently unclear and is of great interest for further studies. One possibility is that the PNJ forms a membrane barrier (Lasiecka et al., 2009; Rosenbluth, 2009) or sieve (Pedraza et al., 2001; Poliak and Peles, 2003; Salzer et al., 2008; Susuki and Rasband, 2008), which depends on the presence of a distinct paranodal cytoskeleton (Ogawa et al., 2006). In accordance with this idea, we have recently found that the interaction of Caspr with the cytoskeletal linker protein 4.1 B at the PNJ is required for the formation of an efficient membrane barrier that segregates between juxtaparanodal K^+ channels and nodal Na^+ channels (Horresh et al., 2010). Our findings that the role of the PNJ in node formation could be revealed only when nodal axon-glial contact is impaired should assist in these further investigations.

Two Distinct Axoglial Adhesion Systems Assemble the Nodes of Ranvier

Our data reveal that Schwann cells control the assembly of nodes of Ranvier by two distinct mechanisms (i.e., clustering and restriction), which operates simultaneously during development. The clustering mechanism requires the establishment of axon-glial contact between Schwann cells microvilli and the axolemma, and is mediated by gliomedin, NrCAM, and NF186. In contrast, the restriction mechanism does not require these three nodal CAMs, and instead depends on axon-glia interaction at the PNJ, which is mediated by Caspr, contactin and NF155. We demonstrated each of the two mechanisms is sufficient for the assembly of mature nodes. For example, in *caspr*$^{-/-}$ mice, Na^+ channels are clustered at heminodes and then in mature nodes, indicating that the heminodal clustering mechanism operates independently from the PNJ and is sufficient to bring Na^+ channels to mature nodes in the absence of this junction. In agreement, Na^+ channels are found in mature nodes in peripheral nerves of several paranodal mutant mice, including *contactin*$^{-/-}$, *cgt*$^{-/-}$, *cst*$^{-/-}$, and *nf155*$^{-/-}$ (Boyle et al., 2001; Dupree et al., 1999; Ishibashi et al., 2002; Pillai et al., 2009). In the absence of heminodal clustering, as observed in *gldn*$^{-/-}$ *nrcam*$^{-/-}$ mice, and *NF186*$^{-/-}$ cultures, Na^+ channels are not clustered at heminodes but nevertheless accumulate in mature nodes that are flanked by PNJs. These results indicate that the clustering mechanism operates at both heminodes and mature nodes, while the PNJ-mediated accumulation of Na^+ channels primarily occurs at mature nodes. It should be emphasized that during PNS node formation, heminodal clustering and PNJ-mediated restriction are likely to work in concert with additional mechanisms that may clear Na^+ channels from beneath the myelin in the internodes (Eshed et al., 2005) and regulate their interaction with the nodal cytoskeletal anchor (Susuki and Rasband, 2008). Interestingly, during their accumulation at nodes in the absence of heminodal clustering, Na^+ channels were invariably associated with ankyrin G and βIV spectrin, both of which were previously shown to have essential roles in organizing and stabilizing the nodes (Dzhashiashvili et al., 2007; Komada and Soriano, 2002). This implies that while heminodal and paranodal mechanisms of node formation require different adhesion complexes, both are likely to depend on the same cytoplasmic anchoring proteins. In conclusion, we show that both heminodal clustering and PNJ-mediated restriction of Na^+ channels take place simultaneously during the development of myelinated peripheral nerves. These two

processes cooperate and provide reciprocal backup systems to ensure that Na^+ channels are found at high density at the nodes.

EXPERIMENTAL PROCEDURES

Generation of Mutant Mice

Gliomedin targeting vector was designed to replace exons 9-10, encoding the olfactomedin domain, with an FRT-PGK-neo-FRT cassette (Gene Bridges). Genomic DNA was cloned from BAC (RPC22 library) by recombineering using the following primers: 3′3′-TAT AAG ATC TCC TTG CCC CAC GTG TTA TCC, 5′3′-AAG ACT CGA GTG ACC CAG TAT CCC TCC TCA A, 3′5′-ACA CCC GCG GGA GGA GGG AGA CTC TTA CCC, 5′5′-TTG TGT CGA CCC GTA ACA CTA ATG TCA TTG. ES cells were electroporated with the linearized targeting construct, and recombinant ES clones were selected with G418. Clones containing correctly targeted integrations were identified by Southern blot analysis, of SalI (5′RM) and BglI (3′RM) digested genomic DNA. Probes were prepared using the following primers:: 3′-CAC CGT GGA CTC ATC TTG GG, 5′-GCC TGT CCC TCT TTA TGC CC, and for the 3′ probe: 3′-GCT AAA CAA CAA ACT GAA TTG AAA C, 5′-CCT ACA TTC TAT GTG GAA TGC TC. Positive ES clones were used to produce chimeric mice by aggregation, as described before (Poliak et al., 2003). Heterozygous *caspr*$^{-/+}$ (Gollan et al., 2003) *nrcam*$^{-/+}$ (Custer et al., 2003) and *nfsac*$^{-/+}$ (Sherman et al., 2005) mice were crossed to generate different double mutants. All lines were backcrossed once to ICR, and analysis was done on F2–F6 generation. At least three mice of each genotype were used for EM and immunofluorescence analysis. All experiments were performed in compliance with the relevant laws and institutional guidelines and were approved by the Weizmann Institute's Animal Care and Use Committee.

Constructs and Antibodies

FC-fusion constructs of gliomedin and NrCAM were described formerly. Rabbit polyclonal antibodies against gliomedin (Eshed et al., 2007), Caspr (Peles et al., 1997), NrCAM (Lustig et al., 2001), mouse monoclonal antibodies against gliomedin (Eshed et al., 2005), and Caspr (Poliak et al., 1999) were all described. Rat antibodies against Caspr and NrCAM were raised against the same antigens as the rabbit antibodies. A rabbit antibody against beta IV spectrin (S1515) and a mouse anti-Nav pan antibody (S8809) were purchased from Sigma Aldrich; mouse anti-ankyrin G (sc 12719) from Santa Cruz Biotechnology; mouse anti-MAG (513) from Roche; rat anti-MBP (MAB386) and rat anti-NF-H (MAB5448) from Chemicon. Rabbit anti- Nav pan antibody (098-21) was kindly provided by Dr. R. Levinson; mouse monoclonal antibody to neurofascin (A4/3.4) was a gift from Dr. M. Rasband.

Electron Microscopy

Mice were anesthetized using a lethal dose of ketamine/xylazine (1:10) injected intraperitoneally. Anesthetized animals were perfused with a fixative containing 4% paraformaldehyde, 2.5% glutaraldehyde, 0.13M NaH_4PO_4, and 0.11M NaOH (pH 7.4). Perfused animals were next incubated in the fixative for 2 weeks at 4°C. Excised sciatic nerves were processed as previously described (Poliak et al., 2003), and were examined using a Philips CM-12 transmission electron microscope.

Immunofluorescence Labeling and Clustering Experiments

Teased sciatic nerves and frozen sections were prepared and immunolabeled as previously described (Poliak et al., 2003). DRG myelinating cultures were fixed in 4% paraformaldehyde for 10 min at RT, and immunolabeled as previously described (Eshed et al., 2005). Clustering experiments on DRG neurons were formerly described as well (Eshed et al., 2005). Fluorescence images were obtained using an Axioskop 2 microscope equipped with Apotom imaging system (Carl Zeiss), or a Nikon eclipse 90i microscope, fitted with a Hamamatsu ORCA-ER CCD camera.

Immunoprecipitation and Immunoblot Analysis

Immunoprecipitation and immunoblot experiments using cell lysates and conditioned media were preformed as previously described (Eshed et al., 2007). For analysis of *gldn*$^{-/-}$ mice, sciatic nerves isolated from adult animals were crushed in liquid nitrogen and homogenized in a buffer containing 95 mM NaCl, 25 mM Tris (pH 7.4), 10 mM EDTA, 2% Triton-X114 and protease inhibitors mix (Sigma). For analysis of Na^+ channels, sciatic nerves of P6 animals were sonicated 3 times for 5 s in an ice-cold sodium pyrophosphate buffer (20 mM tetrasodium pyrophosphate, 20 mM sodium phosphate, 1 mM magnesium chloride, 0.5 mM EDTA, 300 mM sucrose, 1 mM iodacetamide, and protease inhibitors). Tissue homogenates were mixed with 3 volume of 5× Laemmli sample buffer and denatured at room temperature for 10 min.

Tissue Culture Techniques

Dissociated rat DRG myelinating cultures were prepared as described before (Eshed et al., 2005). Briefly, DRGs of E13 genotyped mouse embryos were trypsinized, seeded on Matrigel (BD Biosciences), and Poly-D-Lysine (Sigma Aldrich)-coated 13 mm slides and grown in BN medium containing Basal medium-Eagle, ITS supplement, 0.2% BSA, 4 mg/ml D-glucose (all from Sigma Aldrich), glutamax (GIBCO), 50 ng/ml NGF (Almone Labs), and antibiotics. To induce myelination, cultures were grown in BNC medium, namely a BN medium supplemented with 15% heat inactivated fetal calf serum (replacing the BSA) and 50 μg/ml L-ascorbic acid (Sigma Aldrich) for 12 additional days. Rat Schwann cell cultures and purified DRG neurons were prepared as previously described (Eshed et al., 2005). For the isolation of mouse Schwann cells, DRG of E13 mouse embryos were trypsinized, suspended in NB medium and seeded on 10 cm Matrigel-coated plates. The next day medium was changed to BN, in which the culture was grown for one more week. Cells were next trypsinized, resuspended in Mouse Schwann Cells Proliferation Medium (MSCPM) containing 2/3 SCPM (Spiegel et al., 2007) and 1/3 Rat Schwann cell conditioned medium, and seeded on 10 cm Primeria plates (BD Falcon). The next day cells were incubated with PBS at room temperature until most Schwann cells had detached while fibroblasts remained attached. Schwann cells were resuspended in MSCPM and grown on Poly-L-Lysine (sigma Aldrich)-coated 10 cm plates until confluent. For the generation of DRG neurons/Schwann cells cocultures, confluent Schwann cells grown for 3 days in DMEM with 10% fetal calf serum were trypsinized and added to purified DRG neurons at a density of 2×10^5 cells per slide. After 4–7 days in BN medium, cultures were induced to myelinate using a BNC medium.

Electrophysiology

Sciatic nerves conductivity measurements were performed essentially as described previously (Poliak et al., 2003). Briefly, sciatic nerves were dissected and placed in a temperature controlled recording chamber set to 37°C. The ends of the nerves were drawn into suction electrodes for stimulation and recording of compound action potentials. Signals were amplified, digitized, recorded, and analyzed on a laboratory computer using pClamp10 program (Molecular Devices). At least seven animals of each genotype were sacrificed for evaluation of compound action potential propagation.

Clustering Experiments

The clustering experiments were performed as previously described (Eshed et al., 2005). Briefly, DRG neurons were grown for 17 days on slides coated with 100 μg/ml Poly-D-lysine (Sigma) and 10 μg/ml laminin (Sigma) before binding. The neurons were then incubated with medium containing Fc fusion proteins that were already incubated with Cy3-conjugated anti-human Fc (Jackson Laboratories) as described previously (Gollan et al., 2003), washed once with Neurobasal medium and grown for additional 48 hr before fixing and staining. Quantification was performed using Volocity software (Improvision). Clusters of 0.1–10 μM in size in each field of view were counted. At list seven independent experiments were performed.

Statistical Analysis

In the experiments where multiple samples were compared, statistical significance was determined using a one-way ANOVA test. To further analyze which experimental group differed from the relevant control group, planned comparisons were done by two tails t test, according to Bonferroni correction.

SUPPLEMENTAL INFORMATION

Supplemental Information includes five figures and two tables and can be found with this article online at doi:10.1016/j.neuron.2010.02.004.

ACKNOWLEDGMENTS

We would like to thank Matt Rasband and Rock Levinson for their generous gift of antibodies and valuable comments. This work was supported by grants from the National Multiple Sclerosis Society (RG3594-A-4), the NIH (NINDS grants NS50220 (E.P.) and NS17965 (P.S.), NYS CORE 19772-3784 (P.S.), the Dr. Miriam and Sheldon G. Adelson Medical Research Foundation, the European Community's Seventh Framework Programme (FP7/2007-2013) under grant agreement No. HEALTH-F2-2008-201535, the Shapell Family Biomedical Research Foundation at the Weizmann Institute, the Moskowitz Center for Imaging, and the Wolgin Prize for Scientific Excellence. E.P. is the Incumbent of the Hanna Hertz Professorial Chair for Multiple Sclerosis and Neuroscience.

Accepted: February 3, 2010
Published: February 24, 2010

REFERENCES

Arroyo, E.J., Sirkowski, E.E., Chitale, R., and Scherer, S.S. (2004). Acute demyelination disrupts the molecular organization of peripheral nervous system nodes. J. Comp. Neurol. *479*, 424–434.

Berghs, S., Aggujaro, D., Dirkx, R., Jr., Maksimova, E., Stabach, P., Hermel, J.M., Zhang, J.P., Philbrick, W., Slepnev, V., Ort, T., and Solimena, M. (2000). betaIV spectrin, a new spectrin localized at axon initial segments and nodes of ranvier in the central and peripheral nervous system. J. Cell Biol. *151*, 985–1002.

Berthold, C.H., and Rydmark, M. (1983). Electron microscopic serial section analysis of nodes of Ranvier in lumbosacral spinal roots of the cat: ultrastructural organization of nodal compartments in fibres of different sizes. J. Neurocytol. *12*, 475–505.

Bhat, M.A., Rios, J.C., Lu, Y., Garcia-Fresco, G.P., Ching, W., St Martin, M., Li, J., Einheber, S., Chesler, M., Rosenbluth, J., et al. (2001). Axon-glia interactions and the domain organization of myelinated axons requires neurexin IV/Caspr/Paranodin. Neuron *30*, 369–383.

Boyle, M.E., Berglund, E.O., Murai, K.K., Weber, L., Peles, E., and Ranscht, B. (2001). Contactin orchestrates assembly of the septate-like junctions at the paranode in myelinated peripheral nerve. Neuron *30*, 385–397.

Ching, W., Zanazzi, G., Levinson, S.R., and Salzer, J.L. (1999). Clustering of neuronal sodium channels requires contact with myelinating Schwann cells. J. Neurocytol. *28*, 295–301.

Coman, I., Aigrot, M.S., Seilhean, D., Reynolds, R., Girault, J.A., Zalc, B., and Lubetzki, C. (2006). Nodal, paranodal and juxtaparanodal axonal proteins during demyelination and remyelination in multiple sclerosis. Brain *129*, 3186–3195.

Craner, M.J., Lo, A.C., Black, J.A., and Waxman, S.G. (2003). Abnormal sodium channel distribution in optic nerve axons in a model of inflammatory demyelination. Brain *126*, 1552–1561.

Custer, A.W., Kazarinova-Noyes, K., Sakurai, T., Xu, X., Simon, W., Grumet, M., and Shrager, P. (2003). The role of the ankyrin-binding protein NrCAM in node of Ranvier formation. J. Neurosci. *23*, 10032–10039.

Davis, J.Q., and Bennett, V. (1994). Ankyrin binding activity shared by the neurofascin/L1/NrCAM family of nervous system cell adhesion molecules. J. Biol. Chem. *269*, 27163–27166.

Davis, J.Q., Lambert, S., and Bennett, V. (1996). Molecular composition of the node of Ranvier: identification of ankyrin-binding cell adhesion molecules neurofascin (mucin+/third FNIII domain-) and NrCAM at nodal axon segments. J. Cell Biol. *135*, 1355–1367.

Dugandzija-Novaković, S., Koszowski, A.G., Levinson, S.R., and Shrager, P. (1995). Clustering of Na+ channels and node of Ranvier formation in remyelinating axons. J. Neurosci. *15*, 492–503.

Dupree, J.L., Girault, J.A., and Popko, B. (1999). Axo-glial interactions regulate the localization of axonal paranodal proteins. J. Cell Biol. *147*, 1145–1152.

Dzhashiashvili, Y., Zhang, Y., Galinska, J., Lam, I., Grumet, M., and Salzer, J.L. (2007). Nodes of Ranvier and axon initial segments are ankyrin G-dependent domains that assemble by distinct mechanisms. J. Cell Biol. *177*, 857–870.

Eshed, Y., Feinberg, K., Poliak, S., Sabanay, H., Sarig-Nadir, O., Spiegel, I., Bermingham, J.R., Jr., and Peles, E. (2005). Gliomedin mediates Schwann cell-axon interaction and the molecular assembly of the nodes of Ranvier. Neuron *47*, 215–229.

Eshed, Y., Feinberg, K., Carey, D.J., and Peles, E. (2007). Secreted gliomedin is a perinodal matrix component of peripheral nerves. J. Cell Biol. *177*, 551–562.

Gatto, C.L., Walker, B.J., and Lambert, S. (2003). Local ERM activation and dynamic growth cones at Schwann cell tips implicated in efficient formation of nodes of Ranvier. J. Cell Biol. *162*, 489–498.

Gollan, L., Salomon, D., Salzer, J.L., and Peles, E. (2003). Caspr regulates the processing of contactin and inhibits its binding to neurofascin. J. Cell Biol. *163*, 1213–1218.

Grumet, M. (1997). Nr-CAM: a cell adhesion molecule with ligand and receptor functions. Cell Tissue Res. *290*, 423–428.

Horresh, I., Bar, V., Kissil, J.L., and Peles, E. (2010). Organization of myelinated axons by Caspr and Caspr2 requires the cytoskeletal adapter protein 4.1B. J. Neurosci. *30*, 2480–2489.

Ishibashi, T., Dupree, J.L., Ikenaka, K., Hirahara, Y., Honke, K., Peles, E., Popko, B., Suzuki, K., Nishino, H., and Baba, H. (2002). A myelin galactolipid, sulfatide, is essential for maintenance of ion channels on myelinated axon but not essential for initial cluster formation. J. Neurosci. *22*, 6507–6514.

Kayyem, J.F., Roman, J.M., de la Rosa, E.J., Schwarz, U., and Dreyer, W.J. (1992). Bravo/Nr-CAM is closely related to the cell adhesion molecules L1 and Ng-CAM and has a similar heterodimer structure. J. Cell Biol. *118*, 1259–1270.

Komada, M., and Soriano, P. (2002). [Beta]IV-spectrin regulates sodium channel clustering through ankyrin-G at axon initial segments and nodes of Ranvier. J. Cell Biol. *156*, 337–348.

Kordeli, E., Davis, J., Trapp, B., and Bennett, V. (1990). An isoform of ankyrin is localized at nodes of Ranvier in myelinated axons of central and peripheral nerves. J. Cell Biol. *110*, 1341–1352.

Lambert, S., Davis, J.Q., and Bennett, V. (1997). Morphogenesis of the node of Ranvier: coclusters of ankyrin and ankyrin-binding integral proteins define early developmental intermediates. J. Neurosci. *17*, 7025–7036.

Lasiecka, Z.M., Yap, C.C., Vakulenko, M., and Winckler, B. (2009). Compartmentalizing the neuronal plasma membrane from axon initial segments to synapses. Int. Rev. Cell Mol. Biol. *272*, 303–389.

Lemaillet, G., Walker, B., and Lambert, S. (2003). Identification of a conserved ankyrin-binding motif in the family of sodium channel alpha subunits. J. Biol. Chem. *278*, 27333–27339.

Lonigro, A., and Devaux, J.J. (2009). Disruption of neurofascin and gliomedin at nodes of Ranvier precedes demyelination in experimental allergic neuritis. Brain *132*, 260–273.

Lustig, M., Zanazzi, G., Sakurai, T., Blanco, C., Levinson, S.R., Lambert, S., Grumet, M., and Salzer, J.L. (2001). Nr-CAM and neurofascin interactions regulate ankyrin G and sodium channel clustering at the node of Ranvier. Curr. Biol. *11*, 1864–1869.

Maertens, B., Hopkins, D., Franzke, C.W., Keene, D.R., Bruckner-Tuderman, L., Greenspan, D.S., and Koch, M. (2007). Cleavage and oligomerization of gliomedin, a transmembrane collagen required for node of ranvier formation. J. Biol. Chem. *282*, 10647–10659.

Malhotra, J.D., Kazen-Gillespie, K., Hortsch, M., and Isom, L.L. (2000). Sodium channel beta subunits mediate homophilic cell adhesion and recruit ankyrin to points of cell-cell contact. J. Biol. Chem. *275*, 11383–11388.

McEwen, D.P., and Isom, L.L. (2004). Heterophilic interactions of sodium channel beta1 subunits with axonal and glial cell adhesion molecules. J. Biol. Chem. *279*, 52744–52752.

Melendez-Vasquez, C.V., Rios, J.C., Zanazzi, G., Lambert, S., Bretscher, A., and Salzer, J.L. (2001). Nodes of Ranvier form in association with ezrin-radixin-moesin (ERM)-positive Schwann cell processes. Proc. Natl. Acad. Sci. USA *98*, 1235–1240.

Occhi, S., Zambroni, D., Del Carro, U., Amadio, S., Sirkowski, E.E., Scherer, S.S., Campbell, K.P., Moore, S.A., Chen, Z.L., Strickland, S., et al. (2005). Both laminin and Schwann cell dystroglycan are necessary for proper clustering of sodium channels at nodes of Ranvier. J. Neurosci. *25*, 9418–9427.

Ogawa, Y., Schafer, D.P., Horresh, I., Bar, V., Hales, K., Yang, Y., Susuki, K., Peles, E., Stankewich, M.C., and Rasband, M.N. (2006). Spectrins and ankyrinB constitute a specialized paranodal cytoskeleton. J. Neurosci. *26*, 5230–5239.

Pedraza, L., Huang, J.K., and Colman, D.R. (2001). Organizing principles of the axoglial apparatus. Neuron *30*, 335–344.

Peles, E., Nativ, M., Lustig, M., Grumet, M., Schilling, J., Martinez, R., Plowman, G.D., and Schlessinger, J. (1997). Identification of a novel contactin-associated transmembrane receptor with multiple domains implicated in protein-protein interactions. EMBO J. *16*, 978–988.

Pillai, A.M., Thaxton, C., Pribisko, A.L., Cheng, J.G., Dupree, J.L., and Bhat, M.A. (2009). Spatiotemporal ablation of myelinating glia-specific neurofascin (Nfasc NF155) in mice reveals gradual loss of paranodal axoglial junctions and concomitant disorganization of axonal domains. J. Neurosci. Res. *87*, 1773–1793.

Poliak, S., and Peles, E. (2003). The local differentiation of myelinated axons at nodes of Ranvier. Nat. Rev. Neurosci. *4*, 968–980.

Poliak, S., Gollan, L., Martinez, R., Custer, A., Einheber, S., Salzer, J.L., Trimmer, J.S., Shrager, P., and Peles, E. (1999). Caspr2, a new member of the neurexin superfamily, is localized at the juxtaparanodes of myelinated axons and associates with K+ channels. Neuron *24*, 1037–1047.

Poliak, S., Salomon, D., Elhanany, H., Sabanay, H., Kiernan, B., Pevny, L., Stewart, C.L., Xu, X., Chiu, S.Y., Shrager, P., et al. (2003). Juxtaparanodal clustering of Shaker-like K+ channels in myelinated axons depends on Caspr2 and TAG-1. J. Cell Biol. *162*, 1149–1160.

Rasband, M.N., Peles, E., Trimmer, J.S., Levinson, S.R., Lux, S.E., and Shrager, P. (1999). Dependence of nodal sodium channel clustering on paranodal axoglial contact in the developing CNS. J. Neurosci. *19*, 7516–7528.

Ratcliffe, C.F., Westenbroek, R.E., Curtis, R., and Catterall, W.A. (2001). Sodium channel beta1 and beta3 subunits associate with neurofascin through their extracellular immunoglobulin-like domain. J. Cell Biol. *154*, 427–434.

Rios, J.C., Melendez-Vasquez, C.V., Einheber, S., Lustig, M., Grumet, M., Hemperly, J., Peles, E., and Salzer, J.L. (2000). Contactin-associated protein (Caspr) and contactin form a complex that is targeted to the paranodal junctions during myelination. J. Neurosci. *20*, 8354–8364.

Rios, J.C., Rubin, M., St Martin, M., Downey, R.T., Einheber, S., Rosenbluth, J., Levinson, S.R., Bhat, M., and Salzer, J.L. (2003). Paranodal interactions regulate expression of sodium channel subtypes and provide a diffusion barrier for the node of Ranvier. J. Neurosci. *23*, 7001–7011.

Rosenbluth, J. (1976). Intramembranous particle distribution at the node of Ranvier and adjacent axolemma in myelinated axons of the frog brain. J. Neurocytol. *5*, 731–745.

Rosenbluth, J. (2009). Multiple functions of the paranodal junction of myelinated nerve fibers. J. Neurosci. Res. *87*, 3250–3258.

Saito, F., Moore, S.A., Barresi, R., Henry, M.D., Messing, A., Ross-Barta, S.E., Cohn, R.D., Williamson, R.A., Sluka, K.A., Sherman, D.L., et al. (2003). Unique role of dystroglycan in peripheral nerve myelination, nodal structure, and sodium channel stabilization. Neuron *38*, 747–758.

Salzer, J.L., Brophy, P.J., and Peles, E. (2008). Molecular domains of myelinated axons in the peripheral nervous system. Glia *56*, 1532–1540.

Schafer, D.P., Custer, A.W., Shrager, P., and Rasband, M.N. (2006). Early events in node of Ranvier formation during myelination and remyelination in the PNS. Neuron Glia Biol. *2*, 69–79.

Scherer, S.S., Xu, T., Crino, P., Arroyo, E.J., and Gutmann, D.H. (2001). Ezrin, radixin, and moesin are components of Schwann cell microvilli. J. Neurosci. Res. *65*, 150–164.

Sherman, D.L., Tait, S., Melrose, S., Johnson, R., Zonta, B., Court, F.A., Macklin, W.B., Meek, S., Smith, A.J., Cottrell, D.F., and Brophy, P.J. (2005). Neurofascins are required to establish axonal domains for saltatory conduction. Neuron *48*, 737–742.

Spiegel, I., Adamsky, K., Eshed, Y., Milo, R., Sabanay, H., Sarig-Nadir, O., Horresh, I., Scherer, S.S., Rasband, M.N., and Peles, E. (2007). A central role for Necl4 (SynCAM4) in Schwann cell-axon interaction and myelination. Nat. Neurosci. *10*, 861–869.

Susuki, K., and Rasband, M.N. (2008). Molecular mechanisms of node of Ranvier formation. Curr. Opin. Cell Biol. *20*, 616–623.

Suter, D.M., Pollerberg, G.E., Buchstaller, A., Giger, R.J., Dreyer, W.J., and Sonderegger, P. (1995). Binding between the neural cell adhesion molecules axonin-1 and Nr-CAM/Bravo is involved in neuron-glia interaction. J. Cell Biol. *131*, 1067–1081.

Tait, S., Gunn-Moore, F., Collinson, J.M., Huang, J., Lubetzki, C., Pedraza, L., Sherman, D.L., Colman, D.R., and Brophy, P.J. (2000). An oligodendrocyte cell adhesion molecule at the site of assembly of the paranodal axo-glial junction. J. Cell Biol. *150*, 657–666.

Tao-Cheng, J.H., and Rosenbluth, J. (1983). Axolemmal differentiation in myelinated fibers of rat peripheral nerves. Brain Res. *285*, 251–263.

Vabnick, I., Novaković, S.D., Levinson, S.R., Schachner, M., and Shrager, P. (1996). The clustering of axonal sodium channels during development of the peripheral nervous system. J. Neurosci. *16*, 4914–4922.

Waxman, S.G., and Ritchie, J.M. (1993). Molecular dissection of the myelinated axon. Ann. Neurol. *33*, 121–136.

Zonta, B., Tait, S., Melrose, S., Anderson, H., Harroch, S., Higginson, J., Sherman, D.L., and Brophy, P.J. (2008). Glial and neuronal isoforms of Neurofascin have distinct roles in the assembly of nodes of Ranvier in the central nervous system. J. Cell Biol. *181*, 1169–1177.

Neuron, Volume *65*

Supplemental Information

A Glial Signal Consisting of Gliomedin and NrCAM Clusters Axonal Na^+ Channels during the Formation of Nodes of Ranvier

Konstantin Feinberg, Yael Eshed-Eisenbach, Shahar Frechter, Veronique Amor, Daniela Salomon, Helena Sabanay, Jeffrey L. Dupree, Martin Grumet, Peter J. Brophy, Peter Shrager, and Elior Peles

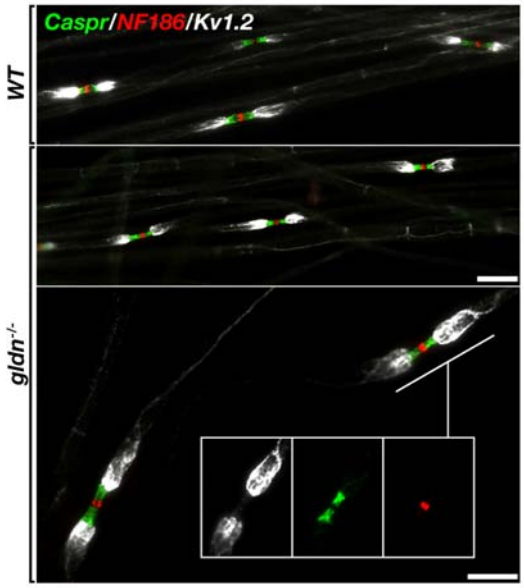

Fig. S1 (*related to Figure 2*). Adult mice lacking gliomedin exhibit normal nodal environs. Nodes (labeled for NF186), PNJs (labeled for Caspr) and juxtaparanodes (labeled for Kv1.2) are present along sciatic nerves of two month-old *gldn*$^{-/-}$ mice similar to their *wt* littermates. Scale bars: upper panel 10μm; lower panel 5μm.

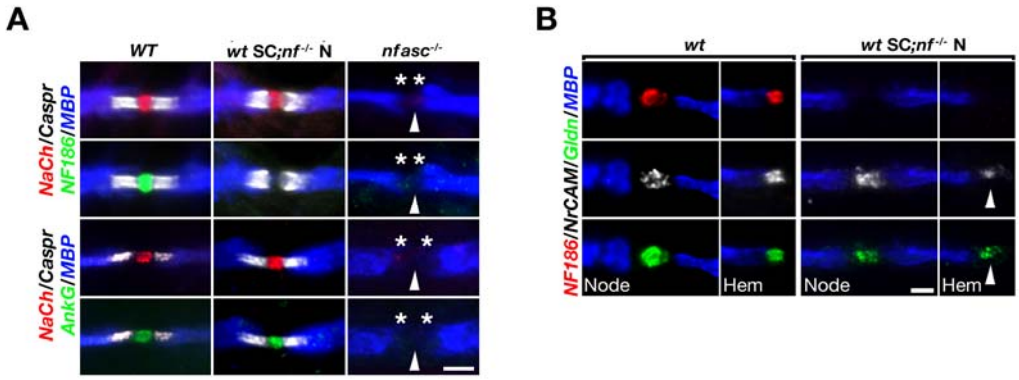

Fig. S2 (*related to Figure 3*). A. Na^+ channels accumulate at nodes in the absence of NF186. Na^+ channels and ankyrin G accumulate at nodes when wild type Schwann cells myelinate neurofascin null (*wt* SC;$nf^{-/-}$ N). Nodes (arrowheads) and PNJs (labeled for Caspr; asterisks) are not formed in $nfasc^{-/-}$ myelinating cultures. Myelin is labeled with an antibody to MBP. **B. Gliomedin and NrCAM are present at heminodes in the absence of NF186.** Myelinated wild type (*wt*) or *wt* SC;$nf^{-/-}$ N cultures were immunolabeled using antibodies to NF186, NrCAM, gliomedin (Gldn) and MBP. Scale bars: A, 5μm; B, 4μm.

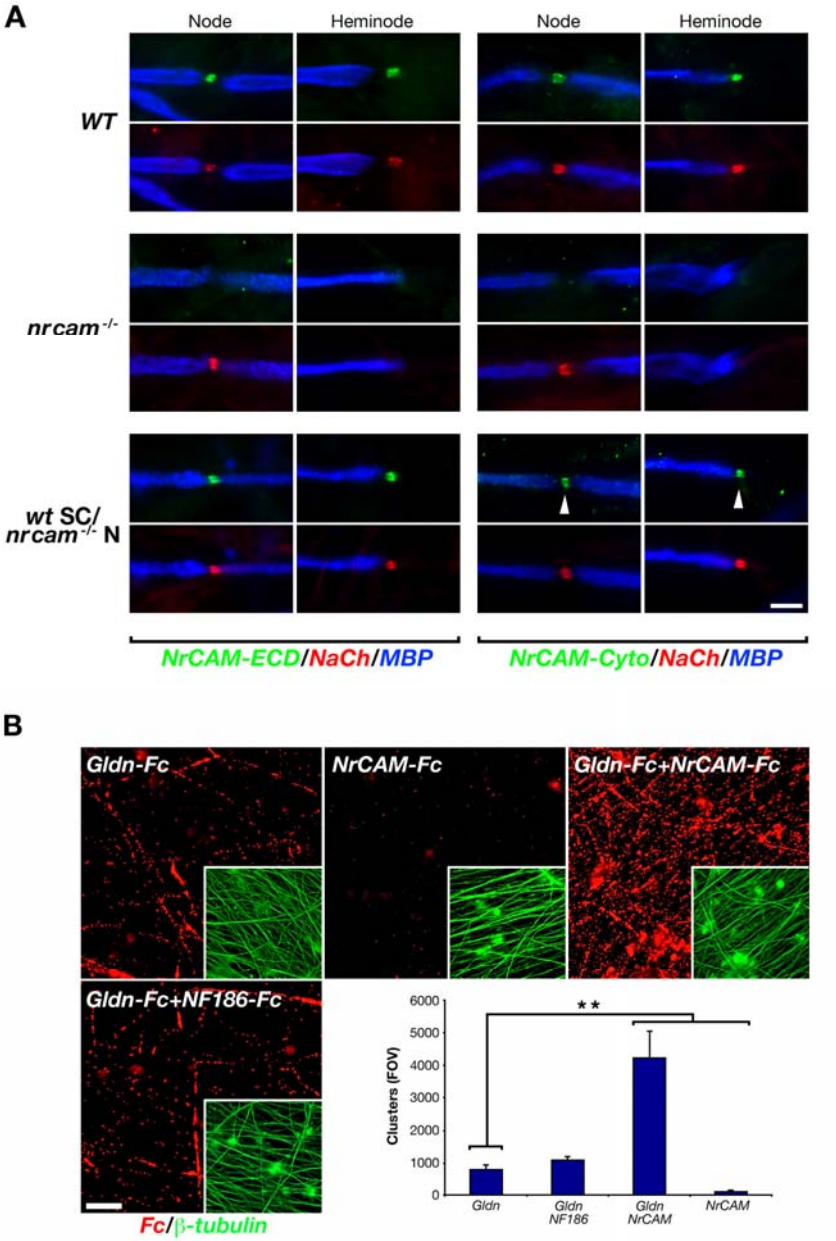

Fig. S3A (*related to Figure 5*). A transmembrane form of glial NrCAM is present at heminodes. Myelinating cultures of DRG neurons and Schwann cells isolated from wild type (*wt*) and nrcam null mice (*nrcam*$^{-/-}$), or cultures containing wild type Schwann cells and *nrcam*$^{-/-}$ neurons (*wt* SC/*nrcam*$^{-/-}$ N), were immunolabeled-using antibodies to Na^{+} channels (NaCh) and MBP together with an antibody directed to the cytoplasmic (NrCAM-Cyto) or the extracellular (NrCAM-ECD) domain of NrCAM. A transmembrane form of NrCAM from glial origin is detected at both nodes and heminodes (arrowheads). **B. NrCAM enhances binding of gliomedin to DRG neurons.** DRG neurons were incubated with the extracellular domain of gliomedin (Gldn-Fc), NrCAM (NrCAM-Fc), a mixture containing both proteins (Gldn-Fc+NrCAM-Fc), or a mixture containing the extracellular domain of gliomedin and NF186 (Gldn-Fc+NF186-Fc). Binding of the Fc-fusion proteins is shown, along with immunolabeling of the cultures with an antibody to bIII tubulin (insets). Quantification of the amount of clusters (surface area) per field of view (FOV) is presented on the right. The experiments were repeated three times. Error bars, SD of *n*=10 fields for each (**p < 0.001). Scale bars: 5μm.

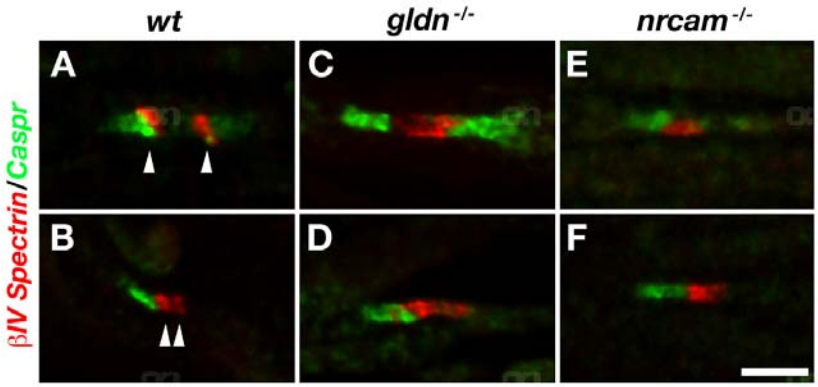

Fig. S4 (*related to Figure 6*). Developmental accumulation of nodal components in *gldn*$^{-/-}$ and *nrcam*$^{-/-}$ mice. Immunolabeling of teased sciatic nerve fibers isolated from six day-old wild type (*wt;* **A-B**), *gldn*$^{-/-}$ (**C-D**), or *nrcam*$^{-/-}$ (**E-F**) mice, using antibodies to βIV spectrin and Caspr. Note that while βIV is clustered at heminodes in the wild type nerve, it is accumulated near Caspr-labeled PNJs in the mutant nerves. Arrowheads mark heminodal clusters in wild type nerves. Scale bar: 5μm.

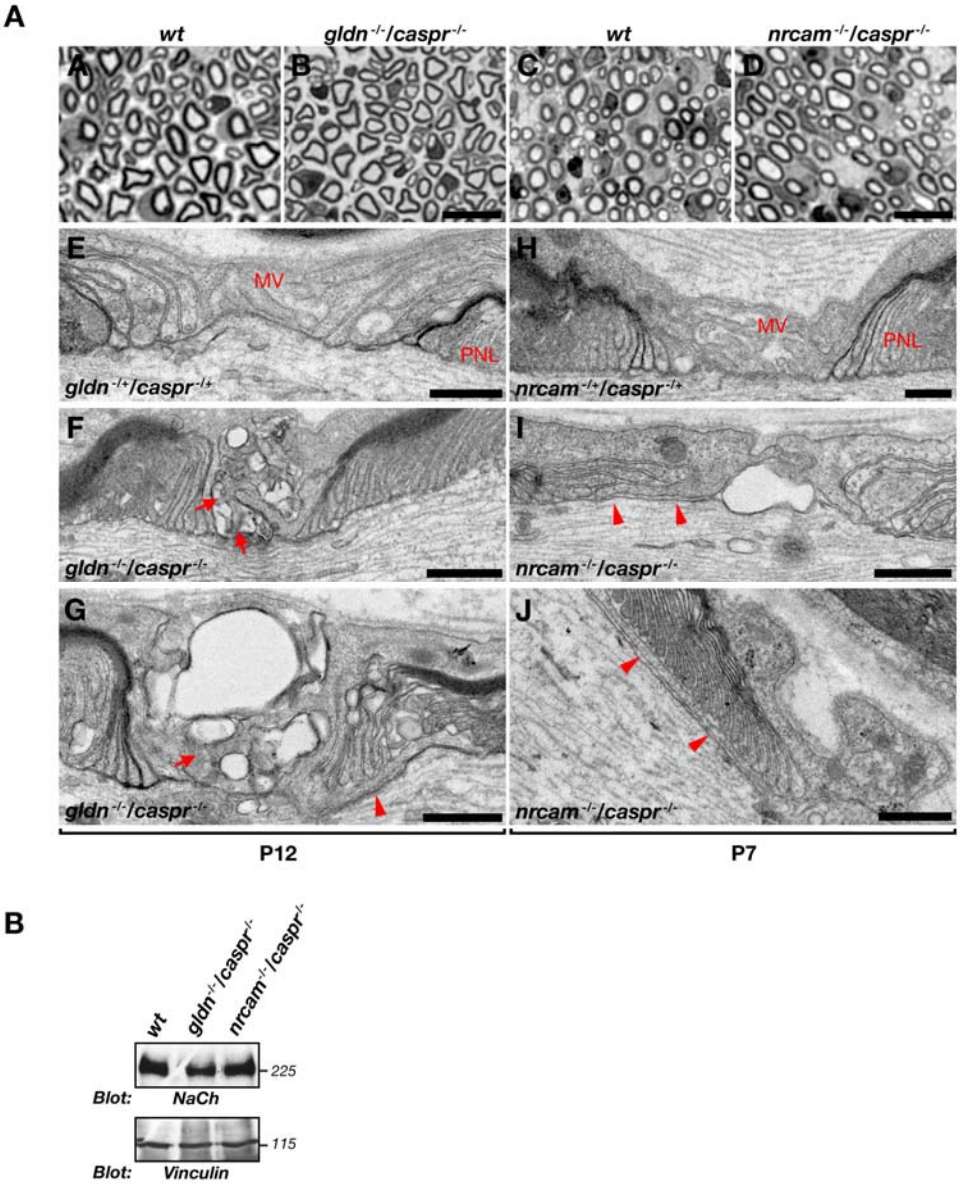

Fig. S5 (*related to Figure 7*). A. Nodal morphology of *gldn*$^{-/-}$/*caspr*$^{-/-}$ and *nrcam*$^{-/-}$/*caspr*$^{-/-}$ mice. Semithin sections showing normal appearance of peripheral myelin in *wt* (**A,C**) and double mutant mice (**B,D**). **E-J.** Electron microscopy images of the nodal area in sciatic nerves isolated from P12 (**E-G**) and P7 (**H-J**) double heterozygous (**E,H**) and double homozygous (**F-G, I-J**) animals. The location of Schwann cell microvilli (MV) and the paranodal loops (PNL) are marked in the first panels. Schwann cell microvilli of *gldn*$^{-/-}$/*caspr*$^{-/-}$ have deteriorated (arrows), and occasionally invade beneath the paranodal loops (arrowheads). In *nrcam*$^{-/-}$/*caspr*$^{-/-}$ nerves the microvilli penetrate the area between the paranodal loops and the axolemma (arrowhead). **B. Expression of Na^{+} channels in sciatic nerves.** Immunoblot analysis of sciatic nerves isolated from P6 wild type (wt), *gldn*$^{-/-}$/*caspr*$^{-/-}$, or *nrcam*$^{-/-}$/*caspr*$^{-/-}$ mice, using antibodies to Na+ channels (NaCh), or vinculin as control. Numbers on the right indicate the location of molecular mass markers in kDa. Scale bars: A-D, 20μm; E-J, 0.5μm.

Genotype	Phenotype	NCV (m/sec)		N	HN
		P7	P14		
wt	Normal	10.2 ± 4.6	19.8 ± 3.2	+	+
***gldn*$^{-/-}$**	Normal	7.4 ± 2.5	20.7 ± 3.9	+	-
***nrcam*$^{-/-}$**	Normal	ND	19.6 ± 2	+	-
***caspr*$^{-/-}$**	Mild ataxia and tremor, normal life span	4.5 ± 3.1	12.8 ± 4.0	+	+
***gldn*$^{-/-}$; *caspr*$^{-/-}$**	Strong congenital ataxia appears at P5, die at P15	ND	8.7 ± 2.4	-	-
***nrcam*$^{-/-}$; *caspr*$^{-/-}$**	Strong congenital ataxia appears at P4, acquired paralysis die at P8	1.5 ± 0.5	ND	-	-
***nfasc*$^{-/-}$**	Paralyzed, die at P7	ND	ND	-	-

Table S1. Summary of the different genotypes used in this study. NCV - nerve conduction velocity; -/+ indicate the formation of normal nodes (N) and heminodes (HN).

Neurons	Schwann	Gldn	NF186	NrCAM	βIV	AnkG	NaCh	Caspr
wt	***wt***	+	+	+	+	+	+	+
***gldn*$^{-/-}$**	***gldn*$^{-/-}$**	-	+	+	+	+	+	+
***nfasc*$^{-/-}$**	***nfasc*$^{-/-}$**	+	-	+	-	-	-	-
***nrcam*$^{-/-}$**	***nrcam*$^{-/-}$**	+	+	-	+	+	+	+
***nfasc*$^{-/-}$**	***wt***	+	-	+	+	+	+	+
***nfasc*$^{-/-}$;*nrcam*$^{-/-}$**	***wt***	-	-	-	+	+	+	+
***nfasc*$^{-/-}$;*nrcam*$^{-/-}$**	***nfasc*$^{-/-}$;*nrcam*$^{-/-}$**	-	-	-	-	-	-	-

Table S2. Nodal composition in myelinated cultures. DRG neurons and Schwann cells isolated from the indicated genotypes were co-cultured. The localization of gliomedin (Gldn), Neurofascin 186 (NF186), NrCAM, βIV spectrin (βIV), ankyrin G (AnkG) and Na^+ channels (NaCh) at nodes, as well as that of Caspr at the PNJ, were determined by immunofluorescence.